B056526

NASA CONTRACTOR REPORT

NASA CR-80

NASA CR-80

PROPERTY OF:

DISTRIBUTION STATEMENT A
Approved for Public Release
Distribution Unlimited

RESEARCH ON PANEL FLUTTER

by D. R. Kobett

Prepared under Contract No. NASr-63(05) *by*
MIDWEST RESEARCH INSTITUTE
Kansas City, Missouri
for

Reproduced From
Best Available Copy

NATIONAL AERONAUTICS AND SPACE ADMINISTRATION • WASHINGTON, D. C. • JULY 1964

56526

RESEARCH ON PANEL FLUTTER

By D. R. Kobett

Prepared under Contract No. NASr-63(05) by
MIDWEST RESEARCH INSTITUTE
Kansas City, Missouri

20011130 116

This report is reproduced photographically
from copy supplied by the contractor.

NATIONAL AERONAUTICS AND SPACE ADMINISTRATION

For sale by the Office of Technical Services, Department of Commerce,
Washington, D.C. 20230 -- Price $2.00

PROPERTY OF:

RESEARCH ON PANEL FLUTTER

By Donald R. Kobett

ABSTRACT

A computer program was developed which is particularly well suited for use in parametric flutter investigations where a large quantity of numerical data is required. The underlying analysis used exact, linearized, three-dimensional aerodynamic theory so the program can be used to investigate the critical low supersonic regime. Finite panel arrays can be treated, and wind tunnel installations can be simulated. A limited quantity of informative numerical data is presented. Most of the data pertains to the flutter of single panels with free side edges, with and without adjacent vertical side walls.

TABLE OF CONTENTS

List of Figures

List of Figures (Concluded)

List of Tables

LIST OF SYMBOLS

(Notation used in the Appendices only is defined at that point and not repeated here)

$A_{m,t}$ = coefficient in Fourier expansion of chordwise deflection function (Eq. (32))

$A_{\bar{m},m}$ = matrix defined in Eq. (38)

a = chord of one panel (Fig. 1)

a_r = defined by Eq. (31)

B = half wavelength in Fourier expansion of spanwise deflection shape (Eq. (23))

$B_{n,u}$ = coefficient in Fourier expansion of spanwise deflection shape (Eq. (23))

$B_{\bar{m},m}$ = matrix defined in Eq. (38)

b = span of one panel (Fig. 1)

b_r = defined by Eq. (31)

$C_{\bar{m},m}$ = matrix defined in Eq. (38)

$C_{m,\bar{\ell}}$ = coefficient in chordwise deflection function (Eq. (17))

$\bar{C}_{n,k}$ = coefficient in spanwise deflection function (Eq. (18))

c_∞ = sound velocity in undisturbed stream

D = $\dfrac{Eh^3}{12(1-\nu^2)}$ = flexural rigidity of panel

$D_{m,\bar{\ell}}$ = coefficient in chordwise deflection function (Eq. (17))

$\bar{D}_{n,k}$ = coefficient in spanwise deflection function (Eq. (18))

E = modulus of elasticity of panel material

$E_{\bar{m},m}$ = matrix defined in Eq. (38)

$F(u)$ = function defined by Eq. (29)

$f_m, \bar{f}_n$ = deflection functions (Eqs.(19,20))

$G_{\bar{m},m,\ell}$ = integral defined by Eq. (36)

g = structural damping coefficient

$H_{\bar{m},m,\ell}$ = integral defined by Eq. (36)

h = panel thickness (dimensional)

$I_{\bar{m},mu}$ = aerodynamic integral (Eq. (35))

$J_{\bar{m},m}$ = structural integral (Eq. (9))

K = kM/β^2

$K_{\bar{m},m}$ = structural integral (Eq. (9))

k = $\frac{\omega a}{U}$ = nondimensional flutter frequency

L = number of chordwise bays in panel array

$\ell, \bar{\ell}$ = integers denoting chordwise panels

M = Mach number

$m, \bar{m}$ = integers denoting chordwise mode number

N = number of spanwise bays in panel array

P_u = function in aerodynamic integral (Eq. (22))

$\bar{p}$ = perturbation pressure at upper surface of panel

p = defined by Eq. (5)

$p_{u,m}$ = defined by Eq. (21)

Q = integral defined in Eq. (9)

q = $\rho U^2/2$ = dynamic pressure

q_m = generalized coordinate

$R_{\bar{m},m}$ = integral defined by Eq. (27)

S = integral defined in Eq. (9)

s = inverse of aspect ratio

T = integral defined in Eq. (9)

T_x = torque per unit length exerted by stringer on panel edge

T_y = torque per unit length exerted by rib on panel edge

t = time

U = free stream velocity

u = index in Fourier expansion (Eq. (23))

w = transverse deflection of panel

x,y,z = reference coordinate system

Z = flutter parameter

$\beta = \sqrt{M^2-1}$

Γ_u = defined in Eq. (22)

γ_m = frequency of m'th chordwise mode

$\bar{\gamma}_n$ = frequency of n'th spanwise mode

ϵ_x = dimensionless coefficient expressing the stringer restraint against rotation

ϵ_y = dimensionless coefficient expressing the rib restraint against rotation

η = local coordinate in spanwise direction

θ = local coordinate in chordwise direction

λ = constant in Fourier expansion of spanwise deflection function (Fig. 3)

λ_r = defined by Eq. (31)

μ = $\tau\rho_s/\rho$ = mass-ratio parameter

ν = Poisson's ratio

ξ = nondimensional chordwise coordinate

ρ = mass density in undisturbed stream

ρ_s = mass density of panel material

τ = h/a = thickness ratio

Φ_m = chordwise deflection function

ϕ = displaced coordinate in Fourier expansion of spanwise deflection shape

Ψ_n = spanwise deflection function

φ = local coordinate

ω = dimensional flutter frequency

I. INTRODUCTION

There is at the present time a serious need for theoretically derived quantitative data on the flutter of flat panels in a supersonic air stream. Aircraft and missile designers need the information as do persons interested in refining the theory by comparison with experimental results. To be generally useful the data must apply to structural configurations of practical interest, and must be extensive enough to differentiate the effects of the numerous nondimensional parameters which characterize the flutter phenomenon.

The flutter problem has been adequately formulated for some time but limited numerical data are available because of the considerable effort required to obtain solutions to the flutter equations. In the present study a computer program was developed which obtains solutions to the flutter equations with relative ease. The program is written for the IBM 7094 computer, and has two significant features:

1. The underlying analysis is broad in scope such that a wide variety of physical conditions is covered. (For example, typical experimental wind tunnel situations can be analyzed.)

2. A technique for the solution of the flutter equations is used which is particularly well suited for parametric studies, i.e., extensive parameter variations can be accomplished with minimum computer effort.

These two features make the computer program of considerable practical value in view of the preceding discussion.

Computations were carried out for some practical physical configurations. Although a relatively small amount of numerical data was gathered because of time limitations, some informative preliminary results were obtained. Of particular interest is a comparison that is made with experimental data for a flat panel with free side edges, front edge clamped and rear edge effectively pinned [6]*. The experimental data give the minimum panel thickness required to prevent flutter as a function of Mach number (M). First mode flutter was observed in all instances. For $M = 1.2$ the present analysis predicts the onset of first mode flutter in good agreement with the experiments. For $M = 1.3$ there is again good agreement between theory and experiment on the onset of first mode flutter. However, for this latter Mach number the theory shows that thicker panels will flutter in the second mode. In other words, the analysis indicates that first mode flutter is not the critical condition, contrary to the experimental findings. These results lead to the conclusion that correlation between theory and experiment needs to be further investigated.

* Numbers in brackets refer to the bibliography.

II. EQUATIONS OF MOTION

In this and the following sections flutter equations of motion are derived for panel arrays of the type shown in Fig. 1.* The panels are geometrically similar with length a and width b. The array extends to an arbitrary number of panels in the chordwise and spanwise directions, and is assumed to be bordered by an inflexible surface extending to infinity. The upper surface $(z > 0)$ is exposed to uniform supersonic flow in the positive x direction while a uniform, steady, pressure equal to the static pressure in the undisturbed stream acts on the lower surface (acoustic effects on the lower surface and membrane stresses due to static pressure difference are not admitted). In the present section, equations of motion are derived in general terms. Specification of boundary conditions and exact formulation of the aerodynamic forces are presented in later sections.

Appropriate equations of motion are obtained by extending the derivation in [1] to include the case of a finite number of panels in the spanwise direction. From small deflection plate theory the equation of motion for the array is

$$D\left[w'^{(4x')} + 2w'^{(2x',2y')} + w'^{(4y')}\right] + \rho_s h w'^{(2t)} + \bar{p}'(x',y',t) = 0 \quad (1)^{**}$$

In Eq. (1) w' is the transverse displacement in the z direction, D the flexural rigidity of the plate, ρ_s the material density, h the plate thickness, and $\bar{p}$ the aerodynamic pressure excess on the side $z > 0$.

Introducing dimensionless quantities x, y, w, $\bar{p}$, and s according to

$$x = x'/a \quad ; \quad y = y'/b$$
$$w = w'/a \quad ; \quad \bar{p} = \bar{p}'/\rho U^2 \qquad (2)$$
$$s = a/b$$

Eq. (1) in dimensionless form becomes

---

* Figures and tables are shown in Appendix A.

** Differentiation is indicated by superscripts in parentheses or brackets. This unconventional notation is adopted to help clarify subsequent formulations.

$$w^{(4x)} + 2s^2 w(2x,2y) + s^4 w^{(4y)} + (\rho_s h a^4/D) w^{(2t)} + (\rho U^2 a^3/D)\bar{p}(x,y,t) = 0 \qquad (3)$$

Solution of (3) is obtained using the Ritz-Galerkin method. In the determination of flutter boundaries a harmonic solution is sought so the deflection is approximated by

$$w = e^{i\omega t} \sum_m q_{m,n} \Phi_m(x) \psi_n(y) \qquad (4)$$

and the pressure is written

$$\bar{p}(x,y,t) = e^{i\omega t} p(x,y) \qquad (5)$$

where the functions $\Phi_m(x)$ and $\psi_n(y)$ satisfy the boundary conditions on the panel.* Following the Ritz-Galerkin method, (4) and (5) are substituted into (3). The resulting equation is multiplied through by $\Phi_{\bar{m}}(x)\psi_n(y)$ and integrated across the length and width of the panel array to give,

$$\sum_m q_{m,n} \left\{ \int_o^L \Phi_m^{(4x)} \Phi_{\bar{m}}\, dx \int_o^N \psi_n^2\, dy + 2s^2 \int_o^L \Phi_m^{(2x)} \Phi_{\bar{m}}\, dx \int_o^N \psi_n^{(2y)} \psi_n\, dy \right.$$

$$\left. + s^4 \int_o^L \Phi_m \Phi_{\bar{m}}\, dx \int_o^N \psi_n^{(4y)} \psi_n\, dy - \left[\frac{\rho_s h a^4 \omega^2}{D}\right] \int_o^L \Phi_m \Phi_{\bar{m}}\, dx \int_o^N \psi_n^2\, dy \right\}$$

$$+ \left[\frac{\rho U^2 a^3}{D}\right] \int_o^L \int_o^N p(x,y) \Phi_{\bar{m}} \psi_n\, dy\, dx = 0 \qquad (6)$$

Now define dimensionless parameters

$$\mu = \tau \rho_s / \rho \qquad (7)$$

$$Z = \tau^3 E / q(1-\nu^2) \qquad (8)$$

* The reason for representing the spanwise dependence of w by a single function $\psi_n(y)$ is discussed later.

where

q = dynamic pressure = $\frac{1}{2}\rho c_\infty^2 M^2$

$\tau = h/a$

M = Mach number

c_∞ = sound velocity in undisturbed stream

E = modulus of elasticity

ν = Poisson's ratio

and let

$$J_{\bar{m},m} = \int_o^L \Phi_m \Phi_{\bar{m}}\, dx$$

$$K_{\bar{m},m} = \int_o^L \Phi_m^{(2x)} \Phi_{\bar{m}}\, dx$$

$$S = \int_o^N \psi_n^2\, dy \tag{9}$$

$$T = \int_o^N \psi_n^{(2y)} \psi_n\, dy$$

$$Q = \int_o^N \psi_n^{(4y)} \psi_n\, dy$$

Substitution of (7), (8), and (9) into (6) yields the set of equations

$$\sum_{\bar{m}} q_{\bar{m},n} \left\{ \frac{Z}{24} \left[\gamma_m^4 J_{\bar{m},m} S + 2s^2 K_{\bar{m},m} T + s^4 J_{\bar{m},m} Q \right] \right.$$

$$\left. - \mu k^2 J_{\bar{m},m} S \right\} + \int_o^L \int_o^N p(x,y) \Phi_{\bar{m}} \psi_n\, dy\, dx = 0 \tag{10}$$

where

$$k = \frac{\omega a}{U}$$

Prior to numerical evaluation of (10) two subsidiary steps are necessary. First the deflection functions $\Phi_m(x)$ and $\psi_n(y)$ must be formulated. Then the aerodynamic integral must be put in a form suitable for computation.

III. THE DEFLECTION FUNCTIONS $\Phi_m(x)$ and $\psi_n(y)$

The deflection functions $\Phi_m(x)$ and $\psi_n(y)$ must satisfy the boundary conditions on the panel array. In the present study two general physical configurations are to be analyzed, each with its own set of boundary conditions. These configurations are:

A. A panel array as pictured in Fig. 1, in which the panel edges are supported by elastic ribs and stringers in the chordwise and spanwise directions, respectively.

B. A panel array with one panel in the spanwise direction (N = 1), with the side edges free and the spanwise edges restrained by stringers as in A.

The deflection functions are formulated for configuration A first.

Configuration A - Boundary conditions for the panel array supported by elastic ribs and stringers are complex and the exact conditions are not treated here. Instead, two simplifying assumptions are introduced as follows:

1. The supporting structure is infinitely rigid in bending, and

2. Torsion is transmitted along the line of a rib (stringer) in the plate only, i.e., the rib (stringer) offers resistance to rotation proportional to local rotation in the plate.

These assumptions retain most of the important physical features and, at the same time, reduce the complexity of the problem. As a consequence of the assumptions the transverse deflections at the edges of the panels are zero and the bending moments are proportional to the slope perpendicular to the edges.

In formulating the boundary conditions along the stringers it is convenient to introduce a local coordinate (Fig. 2).

$$\theta = x-(\bar{\ell}-1) \quad ; \quad \bar{\ell}-1 \le x \le \bar{\ell} \tag{11}$$

and a local chordwise deflection

$$\Phi_m = \Phi_{m,\bar{\ell}}^{(\theta)} \quad ; \quad \bar{\ell} = 1,2,3 \ldots\ldots L \tag{12}$$

The elastic restraints against rotation at the leading and trailing edge stringers are taken as one-half the restraint at the intermediate ones to simplify the formulation. The boundary and compatibility conditions follow from the requirement of zero deflection and continuity of slope and moment at the panel edges.

$$\Phi_{m,\bar{\ell}}(0) = \Phi_{m,\bar{\ell}}(1) = 0 \qquad \bar{\ell} = 1,2,3 \ldots L \quad (13a)$$

$$\Phi^{(\theta)}_{m,\bar{\ell}-1}(1) = \Phi^{(\theta)}_{m,\bar{\ell}}(0) \qquad \bar{\ell} = 2,3 \ldots L \quad (13b)$$

$$\Phi^{(2\theta)}_{m,\bar{\ell}-1}(1) + \epsilon_x \Phi^{(\theta)}_{m,\bar{\ell}-1}(1) = \Phi^{(2\theta)}_{m,\bar{\ell}}(0) - \epsilon_x \Phi^{(\theta)}_{m,\bar{\ell}}(0) \qquad \bar{\ell} = 2,3 \ldots L \quad (13c)$$

$$\Phi^{(2\theta)}_{m,1}(0) = \epsilon_x \Phi^{(\theta)}_{m,1}(0) \quad (13d)$$

$$\Phi^{(2\theta)}_{m,L}(1) = -\epsilon_x \Phi^{(\theta)}_{m,L}(1) \quad (13e)$$

where ϵ_x is a dimensionless coefficient expressing the stringer restraint against rotation.* Equation (13a) requires zero deflection at the stringers and (13b) requires continuity of slope across the stringers. Equation (13c) is a moment balance at the intermediate stringers while (13d) and (13e) are moment balances at the bounding ones.

Boundary conditions along the ribs are formulated in similar manner by introducing local coordinates and spanwise deflection

$$\eta = y-(k-1) \quad ; \quad k-1 \le y \le k \quad (14)$$

and

;

* In terms of dimensional quantities, ϵ_x is given by

$$\epsilon_x = \frac{T_x a}{D\partial w/\partial x}$$

where T_x is the torque per unit length in the stringer and $\partial w/\partial x$ is the slope perpendicular to the stringer.

$$\psi_n = \psi_{n,k}(\eta) \quad ; \quad k = 1,2,3 \ldots N \tag{15}$$

The boundary and compatibility conditions become

$$\psi_{n,k}(0) = \psi_{n,k}(1) = 0 \qquad ; k = 1,2,3 \ldots N \tag{16a}$$

$$\psi^{(\eta)}_{n,k-1}(1) = \psi^{(\eta)}_{n,k}(0) \qquad ; k = 2,3 \ldots N \tag{16b}$$

$$\psi^{(2\eta)}_{n,k-1}(1) + \epsilon_y \psi^{(\eta)}_{n,k-1}(1) = \psi^{(2\eta)}_{n,k}(0) - \epsilon_y \psi^{(\eta)}_{n,k}(0) \quad ; k = 2,3 \ldots N \tag{16c}$$

$$\psi^{(2\eta)}_{n,1}(0) = \epsilon_y \psi^{(\eta)}_{n,1}(0) \tag{16d}$$

$$\psi^{(2\eta)}_{n,N}(1) = - \epsilon_y \psi^{(\eta)}_{n,N}(1) \tag{16e}$$

where ϵ_y is a coefficient expressing the rib restraint against rotation.*

The deflection functions Φ_m and ψ_n are taken to be the natural vibration mode shapes of beams having the boundary conditions (13) and (16), respectively. The natural frequencies and mode shapes of a continuous beam simply supported at equal intervals are given by Miles [2] . Miles' analysis was extended to include restraint against rotation in [1] . This development in [1] is repeated in Appendix B in slightly different form. It is shown that the deflection functions can be written in the form

---

* In terms of dimensional quantities, ϵ_y is given by

$$\epsilon_y = T_y b / D(\partial w/\partial y)$$

where T_y is the torque per unit length in the rib and $\partial w/\partial y$ is the slope perpendicular to the rib.

$$\Phi_{m,\bar{\ell}} = C_{m,\bar{\ell}} f_m(\theta) + D_{m,\bar{\ell}} f_m(1-\theta) \tag{17}$$

and

$$\psi_{n,k} = \bar{C}_{n,k} \bar{f}_n(\eta) + \bar{D}_{n,k} \bar{f}_n(1-\eta) \tag{18}$$

where

$$f_m(\theta) = \sin \gamma_m \theta - \frac{\sin \gamma_m \sinh \gamma_m \theta}{\sinh \gamma_m} \tag{19}$$

$$\bar{f}_n(\eta) = \sin \bar{\gamma}_n \eta - \frac{\sin \bar{\gamma}_n \sinh \bar{\gamma}_n \eta}{\sinh \bar{\gamma}_n} \tag{20}$$

Complete formulations for $\Phi_{m,\bar{\ell}}$ and $\psi_{n,k}$ are given in Appendix B.

Configuration B - Recall that this configuration consists of a panel array as shown in Fig. 1 having one panel in the spanwise direction ($N = 1$), with the side edges free and the spanwise edges restrained by stringers. It is assumed that the panel deflects two-dimensionally, i.e., $\partial w/\partial y = 0$, and therefore that $\psi_n = \psi = 1$. The chordwise deflection function Φ_m is the same as for configuration A.

With the deflection functions Φ_m and ψ_n defined, the integrals of (9) can be readily evaluated in closed form. For these evaluations the reader is referred to Appendix D.

One problem remains in the development of usable flutter equations from (10), namely, integration of the aerodynamic pressure term. This integral is evaluated in the following section.

IV. AERODYNAMIC INTEGRAL

It is required to evaluate the integral

$$\int_o^L \int_o^N p(x,y)\Phi_{\tilde{m}}\psi_n \, dy \, dx$$

from (10), where $p(x,y)$ is the aerodynamic pressure acting on the top surface of the panel array. Since the low supersonic Mach number region is of particular interest, the pressure is obtained from linearized, exact, three-dimensional aerodynamic theory. Use is made of a result from the analysis of Luke and St. John [3] which states that the perturbation pressure on the upper surface for harmonic motion, arbitrary chordwise deflection $\Phi_m(x)$, and sinusoidal spanwise deflection $\sin u\pi\phi/B$ can be written in the dimensionless form*

$$p_{u,m} = \frac{1}{\beta} \sin \frac{u\pi\phi}{\beta} \left\{ \Phi_m^{(x)} + jk\left[(M^2-2)/\beta^2\right]\Phi_m + \int_o^x P_u(\xi)\Phi_m(x-\xi)\, d\xi \right\} \qquad (21)$$

where

$$P_u(\xi) = e^{-jKM\xi} \left\{ -\left[(\Gamma_u{}^2/2) + (k^2/\beta^4)\right]J_o(\Gamma_u\xi) + (\Gamma_u{}^2/2)J_2(\Gamma_u\xi) + j(2k\Gamma_u/\beta^2)J_1(\Gamma_u\xi) \right\} \qquad (22)$$

$$K = kM/\beta^2 \quad ; \quad \Gamma_u{}^2 = K^2 + (u\pi s/B\beta)^2 \quad ; \quad \beta^2 = M^2 - 1$$

and J_n are Bessel functions of the first kind.

The relative simplicity of this result comes from having a deflection shape which extends indefinitely in the spanwise direction. This advantage can be extended to panel arrays of finite spanwise extent by expanding the spanwise deflection shapes ψ_n in a sine series. The total pressure can then

* Bb is the dimensional half wavelength of the spanwise deflection shape.

be expressed as a superposition of terms similar to $p_{u,m}$ in (21). Therefore let the spanwise deflection be represented by

$$\psi_n = \sum_u B_{n,u} \sin u\pi\phi/B \tag{23}$$

The expansion (23), being an odd periodic function, gives ψ_n flanked by periodic reflections. Therefore B is to be chosen such that the reflections are uncoupled aerodynamically, in order to achieve the effect of an isolated finite panel array.* The variable ϕ is the shifted coordinate

$$\phi = y+\lambda$$

where the constant λ depends on B. Criteria for the selection of B and λ are derived in Appendix E.

From (21) and (23) the pressure on the mn'th deflection shape is

$$p_{m,n} = q_{m,n} \sum_u B_{n,u} p_{u,m} \tag{24}$$

and the general pressure term becomes

$$p(x,\phi) = \sum_m p_{m,n} = \sum_m q_{m,n} \sum_u B_{n,u} p_{u,m} \tag{25}$$

After some manipulation the aerodynamic integral from (10) may be written

$$\int_o^L \int_\lambda^{\lambda+N} p(x,\phi)\phi_{\bar{m}}(x)\psi_n(\phi)\, d\phi\, dx = \frac{1}{\beta} \sum_m q_{m,n} \left\{ R_{\bar{m},m} S + jJ_{\bar{m},m} Sk\left[(M^2-2)/\beta^2\right] + \sum_u B_{n,u} F(u) I_{\bar{m},m,u} \right\} \tag{26}$$

* For further discussion of this point see Appendix E and Figs. 3 and 4.

where

$$R_{\bar{m},m} = \int_o^L \Phi_m(x)\Phi_{\bar{m}}(x)\, dx \tag{27}$$

$$I_{\bar{m},m,u} = \int_o^L \int_o^x P_u(\xi)\Phi_m(x-\xi)\Phi_{\bar{m}}(x)\, d\xi\, dx \tag{28}$$

$$F(u) = \int_\lambda^{\lambda+N} \psi_n \sin \frac{u\pi\phi}{B}\, d\phi \tag{29}$$

The integral $R_{\bar{m},m}$ is obtained in closed form by making use of (17) and (19) (see Appendix D). The integral $F(u)$ can also be readily obtained in closed form but it is convenient to momentarily postpone further discussion of this integral.

Two procedures can be used to evaluate $I_{\bar{m},m,u}$.

1. When $\Gamma_u\xi$ and m are small the Bessel functions in $P_u(\xi)$ can be approximated by a sum of circular functions [3] such that

$$P_u(\xi) = \sum_{r=1}^{q} e^{-jKM\xi} \left\{ a_r \cos \lambda_r\xi + jb_r \sin \lambda_r\xi \right\} \tag{30}$$

where

$$\begin{aligned} a_r &= -(1/q)\left[(k^2/\beta^4) + \lambda_r{}^2\right] \\ b_r &= 2k\lambda_r/q\beta^2 \\ \lambda_r &= \Gamma_u \cos\left[(2r-1)/4q\right]\pi \end{aligned} \tag{31}$$

Then if $\Phi_m(x)$ is expanded in a Fourier sine series

$$\Phi_m(x) = \sum_t A_{m,t} \sin (t\pi/L)x \tag{32}$$

$I_{\bar{m},m,u}$ can be evaluated in closed form. Details of this evaluation are given in Appendix C. Roughly speaking this procedure is satisfactory for $m \le 4$, $L \le 2$, and $\Gamma_u \xi \le 10$.

2. When the first procedure is not admissible it is convenient to first change the order of integration to give

$$I_{\bar{m},m,u} = \int_o^L P_u(\xi) \int_\xi^L \Phi_m(x-\xi)\Phi_{\bar{m}}(x)\, dx\, d\xi \tag{33}$$

The integration over x can be completed in closed form. For this purpose introduce another local coordinate similar to (11)

$$\varphi = \xi-(\ell-1) \quad ; \quad \ell-1 \le \xi \le \ell \tag{34}$$

then

$$I_{\bar{m},m,u} = \sum_{\ell=1}^{L} \int_o^1 P_u(\ell-1+\varphi)G_{\bar{m},m,\ell}(\varphi)\, d\varphi$$

$$+ \sum_{\ell=1}^{L-1} \int_o^1 P_u(\ell-1+\varphi)H_{\bar{m},m,\ell}(\varphi)\, d\varphi \tag{35}$$

where

$$G_{\bar{m},m,\ell}(\varphi) = \sum_{\bar{\ell}=\ell}^{L} \int_\varphi^1 \Phi_{m,\bar{\ell}-\ell+1}(\theta-\varphi)\Phi_{\bar{m},\bar{\ell}}(\theta)\, d\theta$$

(36)

$$H_{\bar{m},m,\ell}(\varphi) = \sum_{\bar{\ell}=\ell+1}^{L} \int_o^\varphi \Phi_{m,\bar{\ell}-\ell}(1+\theta-\varphi)\Phi_{\bar{m},\bar{\ell}}(\theta)\, d\theta$$

$G_{\bar{m},m,\ell}$ and $H_{\bar{m},m,\ell}$ are integrated in closed form in Appendix C. The integrations in (35) are evaluated numerically. The first procedure for evaluating $I_{\bar{m},m,u}$ is used in a previously developed computer program for calculating flutter boundaries for panel arrays of infinite spanwise extent. The limitations imposed by the Bessel function approximation (Eq. (30)) prohibit its use on finite span arrays. Consequently, the program developed here makes use of the second procedure.

It remains to evaluate the Fourier coefficients $B_{n,u}$ and the function $F(u)$ introduced in (26) and (29). These quantities depend on both geometrical and aerodynamic details and it is thus appropriate at this point to describe the specific physical situations that are to be analyzed. There are five cases in all:

1. A panel array as shown in Fig. 1 with a finite number of panels in both the chordwise and spanwise direction. The array is bordered by an inflexible surface extending to infinity in all directions.

2. The same as (1) except that the array extends to infinity in the spanwise direction.

3. The same as (1) except that the array is flanked on the sides by vertical walls (a wind tunnel installation for example) an arbitrary distance from the edge of the array.*

4. The same as (1) except that the array has one panel in the spanwise direction (N = 1) and the side edges are free.

5. The same as (4) except that the array is flanked by vertical walls as described in (3).

Cases (1) - (3) conform to the general geometrical configuration A described earlier, while (4) and (5) conform to configuration B. The effect of the vertical walls in (3) and (5) is obtained by introducing image configurations on each side (Fig. 4). For detailed evaluation of $B_{n,u}$ and $F(u)$ the reader is referred to Appendix E.

* The analysis is completed for this option but the option was not programmed because of time limitations.

V. FLUTTER EQUATIONS AND METHOD OF SOLUTION

Flutter equations are obtained from (10) and (26)

$$\sum_m q_m \left\{ \frac{Z}{24} (1+jg) \left[\gamma_m^4 J_{\bar{m},m} S + 2s^2 K_{\bar{m},m} T + s^4 J_{\bar{m},m} Q \right] \right.$$

$$- \mu k^2 J_{\bar{m},m} S + (1/\beta) \left[R_{\bar{m},m} S + j J_{\bar{m},m} S k (M^2-2) / \beta^2 \right.$$

$$\left. \left. + \sum_u B_{n,u} F(u) I_{\bar{m},m,u} \right] \right\} = 0 \qquad (37)$$

In (37) the stiffness terms are multiplied by $(1+jg)$ to account for structural damping.

It is convenient to write (37) in matrix form. Therefore, let

$$\left\{ E_{\bar{m},m} \right\} = \left\{ \gamma_m^4 J_{\bar{m},m} + 2s^2 K_{\bar{m},m} T/S + s^4 Q J_{\bar{m},m}/S \right\}$$

$$\left\{ C_{\bar{m},m} \right\} = \left\{ R_{\bar{m},m} + j J_{\bar{m},m} k (M^2-2)/\beta^2 + A_{\bar{m},m} + j B_{\bar{m},m} \right\}$$

$$\left\{ A_{\bar{m},m} \right\} = \text{Real} \left\{ \sum_u B_{n,u} F(u) I_{m,m,u}/S \right\} \qquad (38)$$

$$\left\{ B_{\bar{m},m} \right\} = \text{Imag} \left\{ \sum_u B_{n,u} F(u) I_{\bar{m},m,u}/S \right\}$$

Then (37) can be written

$$\left\{ \frac{Z}{24} (1+jg) E_{\bar{m},m} - \mu k^2 J_{\bar{m},m} + \frac{1}{\beta} C_{\bar{m},m} \right\} \left\{ q_m \right\} = 0 \qquad (39)$$

where $\left\{ q_m \right\}$ is the flutter vector.

Equation (39) represents a set of simultaneous, homogeneous, algebraic equations. For a nontrivial solution it is necessary to have

$$\text{Det}\left\{\frac{Z}{24}(1+jg)\,E_{\bar{m},m} - \mu k^2 J_{\bar{m},m} + \frac{1}{\beta}\,C_{\bar{m},m}\right\} = 0 \qquad (40)$$

Equation (40) is a concise, mathematical statement of the flutter problem. The computer program must first calculate the elements of the flutter matrix in terms of selected "free" parameters, and then find what combinations of free parameters satisfy (40). Setting up the matrix is straightforward and presents no difficulty. The process of satisfying (40), however, requires some discussion.

On the surface it appears that the free parameters might be any of μ, Z, k and g. The reduced frequency, k, however, is inadmissible since it is contained within $C_{\bar{m},m}$ in complicated transcendental form. Further, it is desirable to make g an input parameter, i.e., to be able to perform flutter calculations for specific values of g. This leaves only the two real parameters μ and Z, and since the flutter determinant of (40) is complex it is necessary that both μ and Z be retained as free parameters. The flutter problem is therefore reduced to one of finding combinations of real μ and Z which satisfy (40), for given input values of g and k.

There is no convenient closed-form type of solution to the posed problem. A conventional approach is to insert specific real values for, say μ, and solve for the Z's which satisfy (40). The Z's so obtained are complex in general and it is necessary to interpolate on μ to find where the imaginary part of Z vanishes. The process is complicated by the fact that for each μ there are m values of Z which satisfy (40). This complication ultimately leads to the necessity to make successive computer runs to obtain flutter points for one set of g,k values.

In the present analysis a solution technique is used which reduces computation time by obtaining flutter points in a single computer run. The method proceeds as follows. For a given value of μ the characteristic equation of the determinant is obtained. This equation is a polynomial in Z with complex coefficients. Assuming Z to be real, the real and imaginary parts are separated into two polynomials

$$a_m Z^m + \ldots\ldots a_1 Z + a_o = 0$$

$$b_m Z^m + \ldots\ldots b_1 Z + b_o = 0 \qquad (41)$$

Any value of Z (with its associated μ) which satisfies both of Eqs. (41) constitutes a flutter point. A modified flutter criterion is therefore obtained, namely that Eqs. (41) have at least one common root. Now (41) will have a common root if and only if the Sylvester determinant formed from the a_i and b_i is zero [4]. This Sylvester determinant is in essence a single-valued function of μ in contrast with the multi-valued function that arises in the conventional approach to the solution. In the present computer program the Sylvester determinant is calculated for a specified array of μ values, and an interpolation procedure is then used to find the exact values of μ for which it vanishes. These μ , with associated Z values, constitute flutter points. The complete process is accomplished in a single computer run.

A computer program has been developed which uses the solution technique just described. Numerical considerations dictate the size of flutter system that can be handled by the program, i.e., the number of chordwise modes, m , that can be used. The present program operates satisfactorily in general for m up to six. Specially tailored routines are used for scaling, determinant evaluation and characteristic equation expansion. It is anticipated that further refinements in these areas, accomplished through selective application of known computational techniques, would extend the range of general application to a greater number of chordwise modes.

VI. NUMERICAL RESULTS

The computer program obtains flutter points in terms of the two general parameters

$$1/\mu = \frac{a\rho}{h\rho_s} = \text{air-panel mass ratio} ,$$

and

$$Z^{1/3} = \frac{h}{a}\left[\frac{E}{q(1-\nu^2)}\right]^{1/3} = \text{stiffness-dynamic pressure ratio}$$

Flutter boundaries can be constructed in the $1/\mu$ - $Z^{1/3}$ plane by making successive calculations for judiciously selected values of reduced flutter frequency k. When only the critical boundary is sought it is still important that a range of k be examined which is extensive enough to locate all the flutter boundaries in the $1/\mu$ - $Z^{1/3}$ plane. If this is not done the boundaries identified as critical may be open to question.

Most of the effort during this contract period went into development of the computer program. Consequently, a limited quantity of numerical data was obtained. Critical flutter boundaries were computed for panel arrays with one chordwise bay (Figs. 6 and 7). Calculations were also carried out for panel arrays with three chordwise bays. These calculations were exploratory ones designed to test the adequacy of the computer program. Finally, calculations were made for panels with free side edges, some in the presence of outboard vertical walls, for comparison with experimental data.

Flutter Boundaries for an Array of Panels

Critical flutter boundaries obtained in a four mode analysis for a panel array consisting of one chordwise bay and an infinite number of spanwise bays are shown in Figs. 6 and 7. Three edge conditions are represented at each of three Mach numbers, for an aspect ratio of 4 and structural damping coefficient of 0.01. The edge condition $\epsilon = 0$ is the pinned condition while $\epsilon = 1{,}000$ closely approximates the clamped case.*

* The pinned edge results were obtained earlier under this contract and are included in [8]. They are repeated here for comparison purposes.

For $M = 1.25$ and 2 the flutter vectors associated with the boundaries are dominated by the first vacuum mode. Coupling with the other modes is present in both cases but is more pronounced for $M = 2$. For $M = \sqrt{2}$ (Fig. 7) the boundaries for $\epsilon = 10$ and 1,000 are also first mode dominant. For $\epsilon = 0$ the critical boundary is composed of three distinct regions. The portion to the right is third mode dominant, the short loop is fourth mode dominant, and the remainder is first mode dominant.

To interpret the results in Figs. 6 and 7 it is best to view values on the abscissa $(1/\mu)$ as denoting specific combinations of panel material, panel thickness, and altitude. Then the ordinate values $(Z^{1/3})$ of points on the boundaries are inversely proportional to the minimum free stream dynamic pressure that will cause flutter. Thus larger $Z^{1/3}$ values correspond to less stable conditions. It is seen in Figs. 6 and 7, that in all cases, decreasing ϵ has a destabilizing effect, i.e., flutter occurs for larger values of $Z^{1/3}$. It is also apparent that the effect of varying ϵ diminishes with increasing Mach number. Finally, comparison of the figures shows that increasing the Mach number has a stabilizing effect.

Six mode analyses were conducted for pinned edge panel arrays with three chordwise bays and an infinite number of spanwise bays. These calculations were intended primarily to assess the adequacy of the computer program. They were not extensive enough to permit the identification of critical boundaries and therefore no detailed results are given here.

Flutter Boundaries for a Single Finite Panel

Some calculations were carried out for comparison with the experimental data in [6] and the analytical results in [7]. The experimental data are for a panel with free side edges, front edge clamped and rear edge effectively pinned. There is a gap between the side edges and the wind tunnel wall equal to 6.2 per cent of the panel span. Aspect ratios vary between 0.95 and 1.06. The analysis [7] treats the case of a panel with side edges free and does not include the effect of the wind tunnel wall. In both [6] and [7], results are presented in the form of thickness-to-prevent-flutter as a function of Mach number.

Two types of calculations were made here, namely, for

(a) A panel with side edges free surrounded by a quiescent surface as in [7], and

(b) A panel with side edges free, flanked by vertical sidewalls to simulate a wind tunnel installation.

Four mode analyses were conducted using the first four natural vibration modes of a two-dimensional beam. Twenty terms are carried in the Fourier expansion of the spanwise deflection shape. (Typical twenty term representations are shown in Fig. 8). All calculations are for an aspect ratio of unity and a structural damping coefficient of 0.01 (approximately the mean experimental values). The experimental edge conditions are not duplicated exactly since the present analysis assumes that edge conditions at the front and rear of the panel are the same. Instead, results are obtained for pinned ($\epsilon = 0$) and clamped ($\epsilon = 1{,}000$) conditions to bracket the experimental conditions.

The calculations were carried out first for configuration (a) at $M = 1.2$. The following critical thickness ratios (τ_{crit}) and frequencies were obtained.

ϵ	τ_{crit}	k*	Dominant Mode
0	0.00465	0.134	1
1,000	0.00424	0.275	1

These points agree remarkably well with the experimental results for $M = 1.2$, namely,

$$\tau_{crit} = 0.00438$$

$$k = 0.187$$

For this same case the analysis [7] gives $\tau_{crit} = 0.0053$ at a frequency "slightly below the second natural frequency." It is seen that the present results agree better with the experimental data than with [7], even though the tunnel walls are not simulated.

Calculations were next carried out for configuration (a) at $M = 1.3$. The following results were obtained.

---

* Exact values of k are not determined by calculation since τ_{crit} is obtained by finding where the critical boundary intersects the line in the $1/\mu - Z^{1/3}$ plane denoting experimental conditions. The values given for k come from linear interpolation between calculated points on each side of the intersection.

ϵ	τ_{crit}	k	Dominant Mode
0	0.00564	0.61	2
1,000	0.00426	0.73	2

For this case the experimental results are

$$\tau_{crit} = 0.00335$$

$$k = 0.165$$

and the analysis [7] gives $\tau_{crit} = 0.0038$ and frequency "slightly below the third natural frequency."

The failure to agree with the experimental data for this case prompted a closer look at the numerical data. It was noted that subcritical boundaries associated with the first chordwise mode are present in the region of general interest. It was not possible to run additional calculations to determine exactly where these boundaries intersect the experimental condition line. However, reasonable extrapolation yields the following thickness ratios:

ϵ	τ
0	0.0036
1,000	0.0032

The corresponding reduced flutter frequencies cannot be obtained by extrapolation but it can be seen that they are less than 0.25. These values of τ and k again compare well with the experimental data.

Calculations were next carried out for configuration (b) to assess the effect of the wind tunnel walls. The following case was investigated.

$$M = 1.3$$

$$\text{aspect ratio} = 1$$

$$g = 0.01$$

gap to wall = 5 per cent of span

edge conditions = pinned; clamped

The 5 per cent gap is smaller than the actual gap in the experimental setup (6.2 per cent). It was so taken to allow for the boundary layer displacement thickness effect. The following results were obtained

ϵ	τ_{crit}	k	Dominant Mode
0	0.0060	0.65	2
1,000	0.0046	0.80	2

The presence of the walls is seen to increase τ_{crit} by about 10 per cent, i.e., the walls have a slight destabilizing effect. Examination of the numerical data again revealed the presence of subcritical boundaries associated with the first mode, but extrapolation of the boundaries was not attempted.

The results that have just been described are summarized below for clarity.

Source of Data	Mach No.	Edge* Cond.	Thickness Ratio	Freq.	Dominant Mode	Gap to* Wall	Critical Cond.
Present	1.2	P	0.00465	0.134	1	-	Yes
"	1.2	C	0.00424	0.275	1	-	"
[6]	1.2	P-C	0.00438	0.187	1	6.2%	"
[7]	1.2	P-C	0.00530	-	2	-	"
Present	1.3	P	0.00564	0.61	2	-	"
"	1.3	C	0.00426	0.73	2	-	"
[6]	1.3	P-C	0.00335	0.165	1	6.2%	"
[7]	1.3	P-C	0.0038	-	3	-	"
Present	1.3	P	0.0036	k<0.25	1	-	No
"	1.3	C	0.0032	k<0.25	1	-	"
"	1.3	P	0.0060	0.65	2	5%	Yes
"	1.3	C	0.0046	0.80	2	5%	"

* Under edge conditions, P indicates pinned, C clamped, and P-C the experimental conditions of front clamped and rear pinned. The gap to wall is given in per cent of panel span.

The above results must be considered as preliminary, subject to a more definitive numerical study. Calculations should be made for additional reduced frequencies to insure that the points identified as critical are truly critical. Experience has shown that it is sometimes easy to miss a complete boundary, which may be the critical one, even though a well chosen range of frequencies is used.* In this light the case $M = 1.2$ should be thoroughly examined for the presence of a critical second mode boundary. Additional calculations should also be made to examine the convergence of the Galerkin procedure and of the Fourier expansion of the spanwise deflection shape.

Estimates of Computing Time

During the course of the calculations, estimates were made of computing time. To present these estimates in a meaningful way, it is necessary first to describe the calculation procedure. A set of input parameters is selected first. Included are

1. Geometry Code**
2. Aspect Ratio
3. Mach number
4. Edge conditions (ϵ)
5. Number of chordwise modes
6. Number of terms in expansion of spanwise deflection shape
7. Damping coefficient, g
8. Frequency, k

A run on the computer consists in loading the data corresponding to inputs 1 through 7 and then cycling through a sequence of frequency values. The total

* This difficulty of choosing reduced frequencies is not unique to the present analysis; it is common to all analyses that make use of exact, three-dimensional aerodynamic theory.

** Geometry code identifies the situation to be analyzed; for instance, an isolated panel with free side edges.

time for a run is comprised of two separable parts. There is a setup time during which matrices that do not depend on frequency are calculated and stored, and there is the time required to process each frequency.

The number of flutter points that are obtained varies from frequency to frequency and the running time varies accordingly. For the four mode calculations that were made for the single panel with free side edges the following averages were obtained.

Set-up time - 0.5 min.

Time per frequency - 0.4 min.

Flutter points per frequency - 3

A few runs made using six chordwise modes indicate that setup time approximately doubles and running time for each frequency increases by a factor of about 2-1/2.

For the runs using six chordwise modes for a panel array with three chordwise bays, the setup time was about 4 min. and the running time for each frequency about 1 to 1-1/4 min. The average number of flutter points per frequency was between 4 and 5.

VII. CONCLUSIONS AND RECOMMENDATIONS

A computer program has been developed which has three significant features:

1 It uses a solution technique that obtains flutter points in a single computer run.

2 It can handle up to six-by-six flutter determinants.

3 It can be used to investigate a variety of physical situations, including that of a single panel installed in a wind tunnel.

Preliminary numerical results suggest the possibility of obtaining meaningful comparison with experiment.

The computer program should be exploited by using it in a definitive parametric investigation of the flutter of flat panel arrays.

An attempt should be made to extend the capability of the computer program to ten-by-ten systems, by refining the implicit numerical operations.

REFERENCES

1. Zeydel, E. F. E., and D. R. Kobett, "Effects of External Force Excitation on Panel Flutter," AFOSR Technical Report, Contract No. AF 49(638)-389, December 1962.

2. Miles, J. W., "Vibrations of Beams on Many Supports," Proceedings, ASCE, Vol. 82, No. EM-1 (1956).

3. Luke, Y. L., and A. D. St. John, "Supersonic Panel Flutter," WADC Tech. Report 57-252, July, 1957.

4. Bocher, M., "Introduction to Higher Algebra," The Macmillan Company (1936).

5. Felgar, R. P., Jr., "Formulas for Integrals Containing Characteristic Functions of a Vibrating Beam," University of Texas, Bureau of Engineering Research Circular No. 14 (1950).

6. Lock, M. H., and Y. C. Fung, "Comparative Experimental and Theoretical Studies of the Flutter of Flat Panels in a Low Supersonic Flow," AFOSR TN 670, May 1961.

7. Cunningham, H. J., "Flutter Analysis of Flat Rectangular Panels Based on Three-Dimensional Supersonic Potential Flow," AIAA Journal, Vol. 1, No. 8, August 1963.

8. Kobett, D. R., and E. F. E. Zeydel, "Research on Panel Flutter," NASA TN D-2227, November 1963.

APPENDIX A

FIGURES 1 THROUGH 8 AND TABLE I

TABLE A-I

COMPARISON BETWEEN PARTIALLY CLAMPED FREQUENCIES AND CLAMPED FREQUENCIES (L = 1)

Mode	ϵ	Partially Clamped Frequency (ϵ) / Clamped Frequency ($\epsilon = \infty$)
1	0	0.441
2	0	0.640
3	0	0.735
4	0	0.790
1	10	0.772
2	10	0.810
3	10	0.838
4	10	0.859
1	100	0.963
2	100	0.964
3	100	0.965
4	100	0.966
1	1,000	0.996
2	1,000	0.996
3	1,000	0.996
4	1,000	0.996

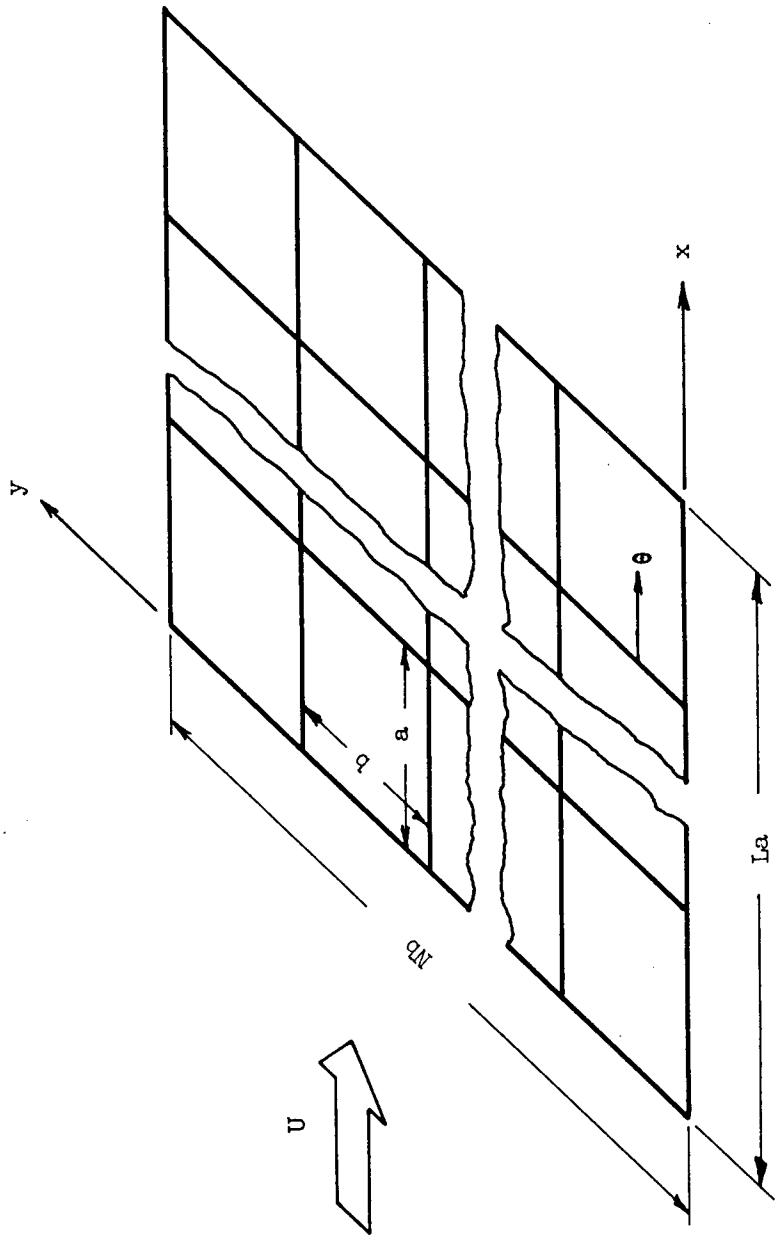

Fig. 1 - Panel Array

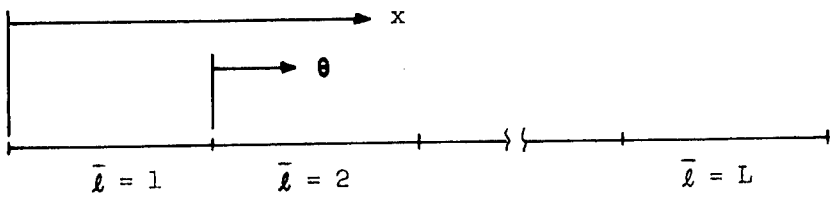

(a) Chordwise Direction

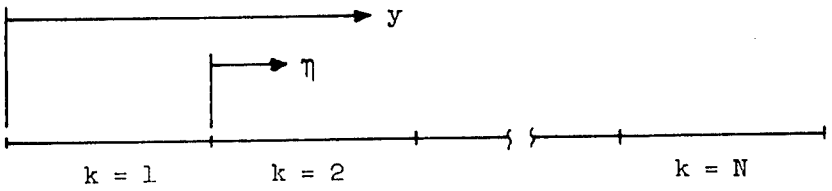

(b) Spanwise Direction

Fig. 2 - Local Coordinates

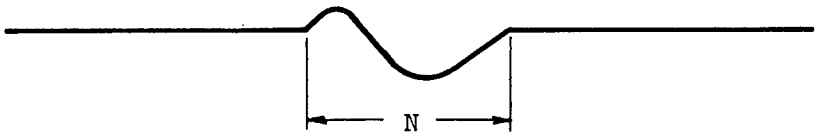

(a) Actual Deflection Shape

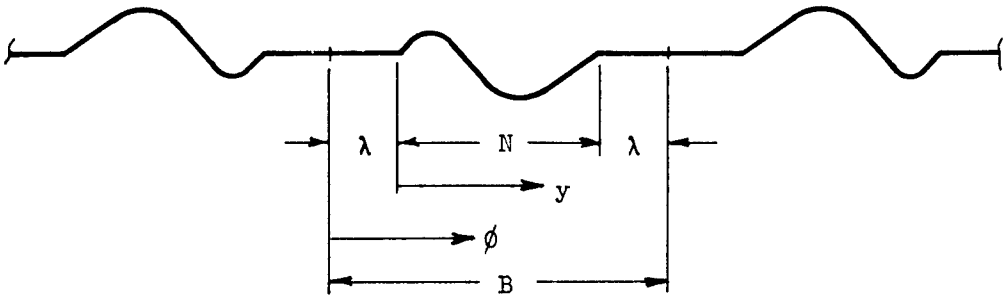

(b) Analytical Deflection Shape

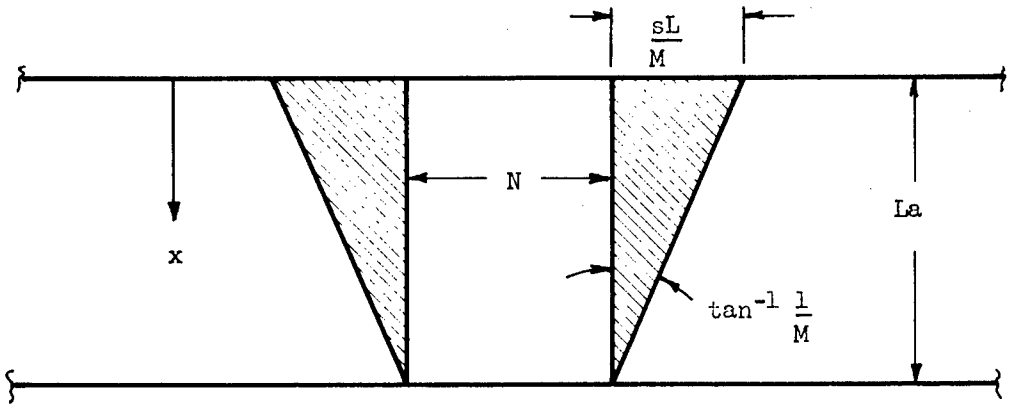

(c) Plan View Showing Maximum Spanwise Excursion of Forward Facing Mach Cone (Shaded Area)

Fig. 3 - Geometrical Aspects of Spanwise Deflection Expansion

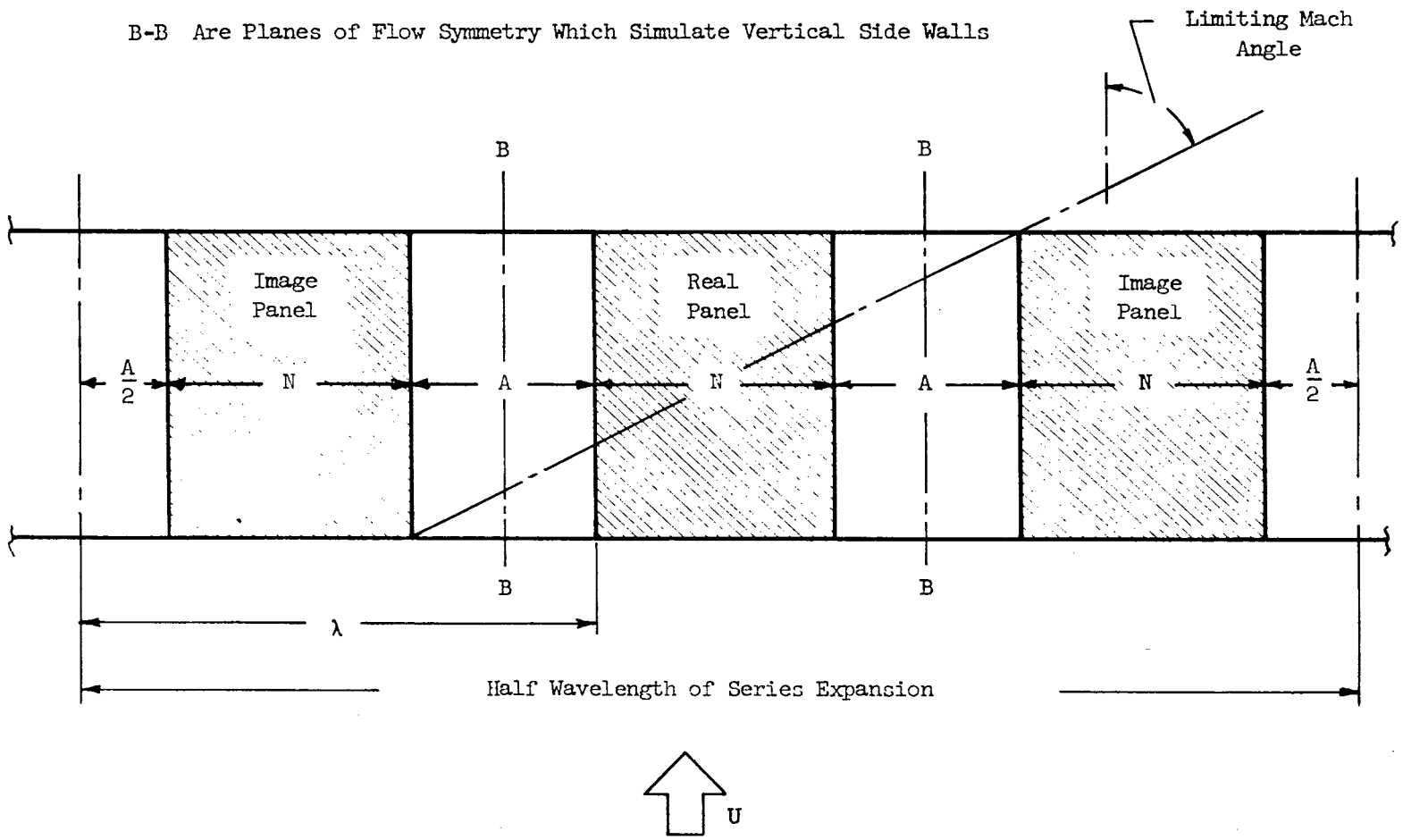

Fig. 4 - Image Panel Configuration

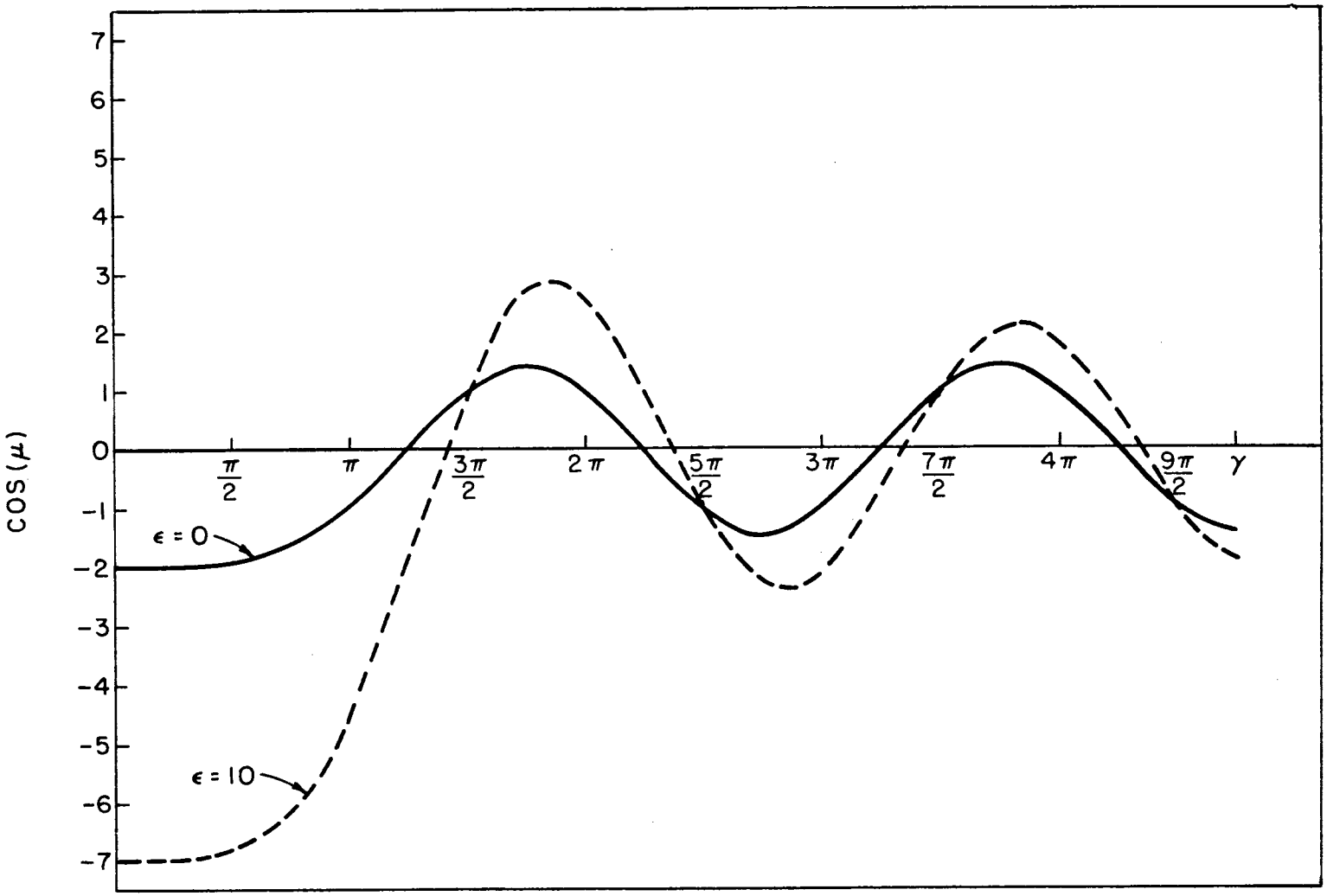

Fig. 5 - Natural Frequencies for a Uniform Beam on Many Supports with Elastic Restraint Against Rotation

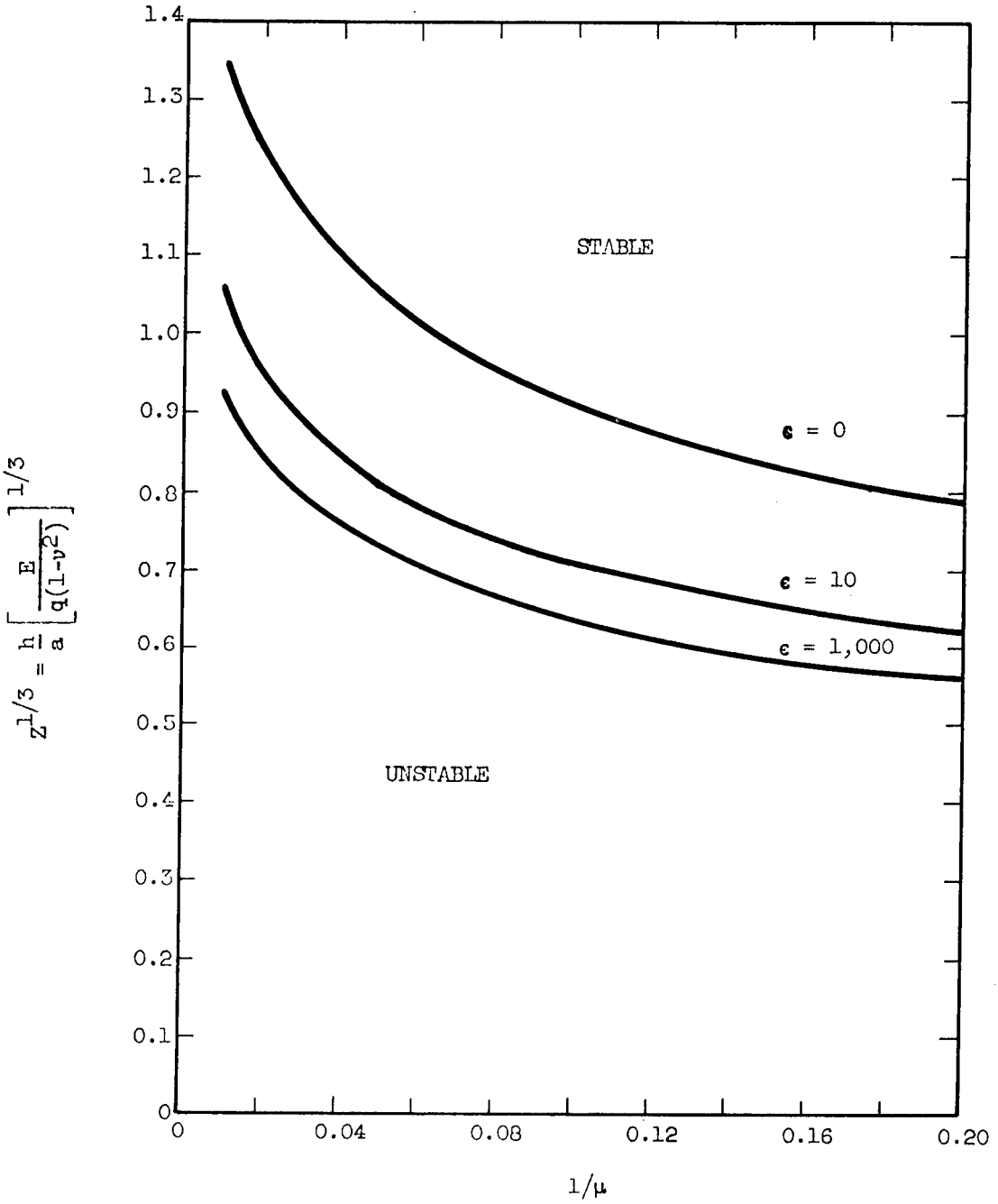

Fig. 6 - Critical Flutter Boundaries from Four Mode Analysis;
M = 1.25, s = 1/4, L = 1, g = 0.01

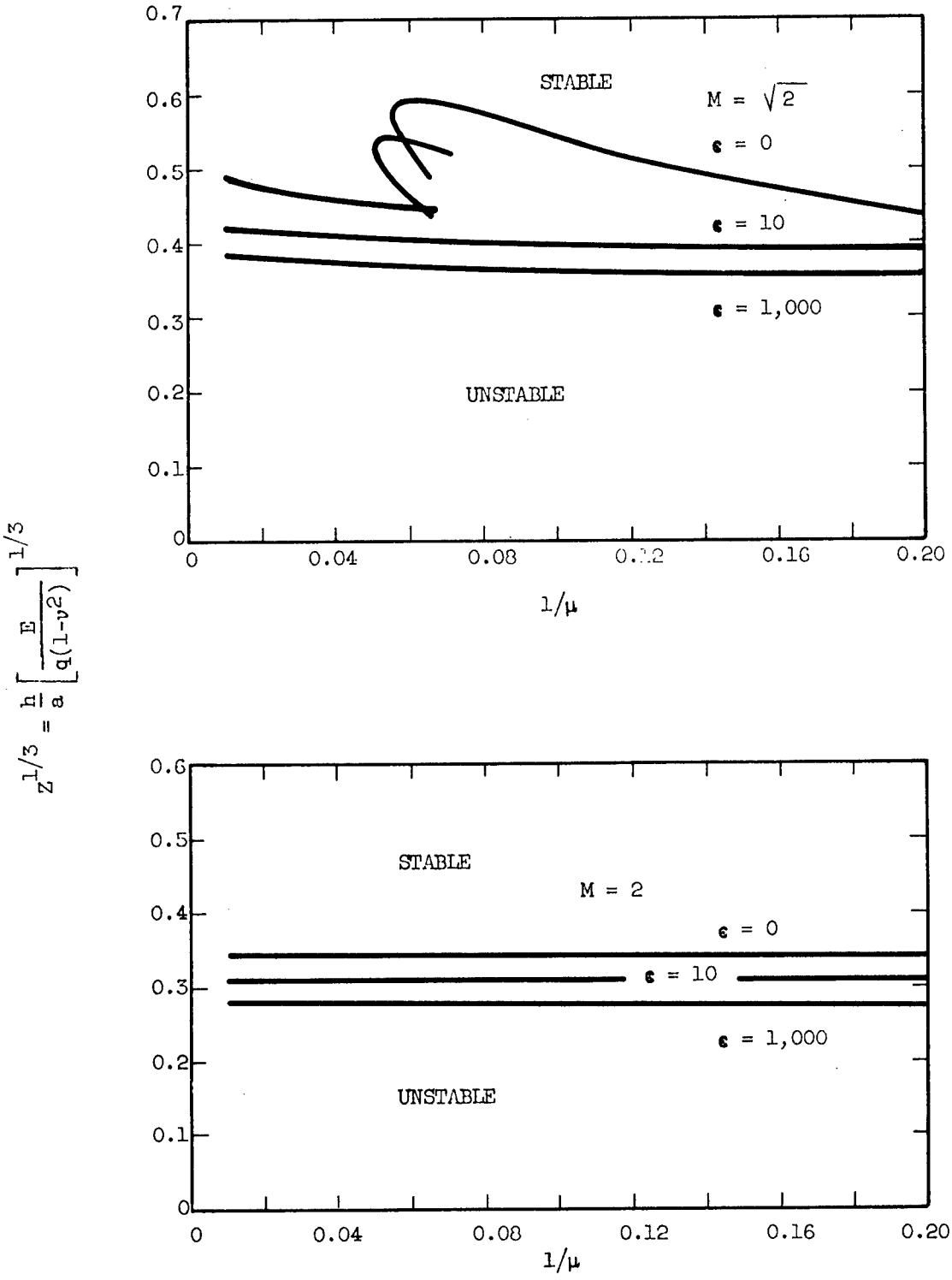

Fig. 7 - Critical Flutter Boundaries from Four Mode Analysis;
s = 1/4, L = 1, g = 0.01

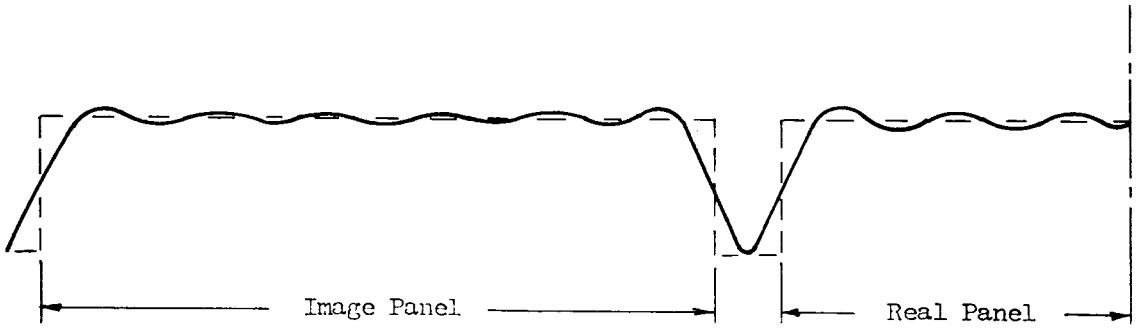

(a) Case 5; Gap to Wall = 5 Per Cent of Panel Span

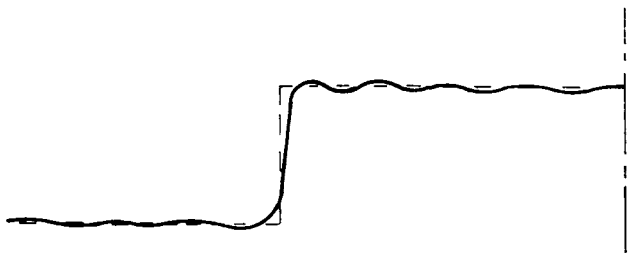

(b) Case 4; M = 1.2, s = 1, L = 1

Fig. 8 - Fourier Expansions (Dashed Line is Shape to be Represented; One-Half Wavelength Shown)

APPENDIX B

EQUATIONS OF MOTION OF A UNIFORM BEAM ON MANY SUPPORTS WITH ELASTIC RESTRAINT AGAINST ROTATION

In this Appendix, Miles' analysis of a continuous beam on equally spaced supports [2] , is extended to include the effects of elastic restraints against rotation at the supports.* The equation of motion of a uniform beam in harmonic motion is

$$\Phi^{(4x)} = \lambda^4 \Phi \tag{B-1}$$

In the formulation of the boundary conditions for a beam supported at $x = 0$, a, $2a$, ... La, it is convenient to introduce a dimensionless local coordinate

$$\theta = \frac{x}{a} - (\bar{\ell}-1) \qquad (\bar{\ell}-1)a \le x \le \bar{\ell}a \tag{B-2}$$

so that

$$\Phi(\theta) = \Phi_{\bar{\ell}}(\theta) \qquad \bar{\ell} = 1,2,3 \ldots L \tag{B-3}$$

where $\gamma^4 = \lambda^4 a^4$.

Taking the elastic restraints against rotation at the intermediate supported edges twice as large as the elastic restraint at the end points, the boundary conditions are

$$\Phi_{\bar{\ell}}(0) = \Phi_{\bar{\ell}}(1) = 0 \qquad \bar{\ell} = 1,2,3 \ldots L \tag{B-4}$$

$$\Phi^{(\theta)}_{\bar{\ell}-1}(1) = \Phi^{(\theta)}_{\bar{\ell}}(0) \qquad \bar{\ell} = 2,3,4 \ldots L \tag{B-5}$$

$$\Phi^{(2\theta)}_{\bar{\ell}-1}(1) + \epsilon\Phi^{(\theta)}_{\bar{\ell}-1}(1) = \Phi^{(2\theta)}_{\bar{\ell}}(0) - \epsilon\Phi^{(\theta)}_{\bar{\ell}}(0) \qquad \bar{\ell} = 2,3,4 \ldots L \tag{B-6}$$

$$\Phi^{(2\theta)}_{1}(0) = \epsilon\Phi^{(\theta)}_{1}(0) \; ; \; \Phi^{(2\theta)}_{L}(1) = - \epsilon\Phi^{(\theta)}_{L}(1) \tag{B-7}$$

---

* The development given here is nearly identical with that given in Appendix B of [1] , the principal difference being in the general form that is selected for the deflection shapes.

where ϵ is a dimensionless coefficient expressing the stiffness of restraint of the edge supports.*

A general solution of (B-3) satisfying (B-4) can be written as

$$\Phi_{\bar{\ell}}(\theta) = C_{\bar{\ell}}\left[\sin \gamma\theta - (\sin \gamma \sinh \gamma\theta)/\sinh \gamma\right]$$

$$+ D_{\bar{\ell}}\left[\sin \gamma(1-\theta) - \left(\sin \gamma \sinh \gamma(1-\theta)\right)/\sinh \gamma\right] \qquad \text{(B-8)}$$

Substitution of (B-8) into (B-5), (B-6), and (B-7) gives

$$C_{\bar{\ell}} - pD_{\bar{\ell}} = pC_{\bar{\ell}-1} - D_{\bar{\ell}-1} \qquad \bar{\ell} = 2,3,4 \ldots L \qquad \text{(B-9)}$$

$$qC_{\bar{\ell}} + D_{\bar{\ell}} = C_{\bar{\ell}-1} + qD_{\bar{\ell}-1} \qquad \bar{\ell} = 2,3,4 \ldots L \qquad \text{(B-10)}$$

$$qC_1 + D_1 = 0 \qquad \text{(B-11)}$$

$$C_L + qD_L = 0 \qquad \text{(B-12)}$$

where

$$p = \left[\sinh \gamma - \sin \gamma\right]^{-1}\left[\sinh \gamma \cos \gamma - \sin \gamma \cosh \gamma\right] \qquad \text{(B-13)}$$

$$q = \left[2\gamma \sin \gamma \sinh \gamma - \epsilon(\sinh \gamma \cos \gamma - \sin \gamma \cosh \gamma)\right]^{-1}$$

$$\times \left[\epsilon(\sinh \gamma - \sin \gamma)\right] \qquad \text{(B-14)}$$

It is convenient to note for later use, that the conditions $q = \pm 1$ give modes that are identical with those of a single span of length a, namely

* See the report body for details of ϵ.

$$\Phi_{\bar{\ell}}(\theta) = q^{(\bar{\ell}-1)}\left[\sin \gamma\theta - (\sin \gamma \sinh \gamma\theta)/\sinh \gamma\right]$$

$$- q^{\bar{\ell}}\left[\sin \gamma(1-\theta) - \left(\sin \gamma \sinh \gamma(1-\theta)\right)/\sinh \gamma\right] \qquad \text{(B-15)}$$

It can be readily verified that (B-15) satisfies (B-9) through (B-12).

Continuing with the general development, Eq. (B-9) and (B-10) can be operated upon to give

$$C_{\bar{\ell}}(1-pq) = 2pD_{\bar{\ell}} - D_{\bar{\ell}-1}(1+pq) \qquad \text{(B-16)}$$

$$D_{\bar{\ell}+1} - 2 \cos \mu \, D_{\bar{\ell}} + D_{\bar{\ell}-1} = 0 \qquad \text{(B-17)}$$

where

$$\cos \mu = \frac{p+q}{pq+1} \quad . \qquad \text{(B-18)}$$

The general solution of (B-17) is

$$D_{\bar{\ell}} = A \cos \bar{\ell}\mu + B \sin \bar{\ell}\mu \qquad \text{(B-19)}$$

and from (B-16) there follows

$$C_{\bar{\ell}} = \frac{1}{1-pq}\left\{2p\left[A \cos \bar{\ell}\mu + B \sin \bar{\ell}\mu\right]\right.$$

$$\left. - (1+pq)\left[A \cos (\bar{\ell}-1)\mu + B \sin (\bar{\ell}-1)\mu\right]\right\} \qquad \text{(B-20)}$$

Substituting (B-19) and (B-20) back into (B-11) and (B-12) gives, after some algebraic manipulation,

$$A(\cos \mu - q) + B \sin \mu = 0 \qquad \text{(B-21)}$$

$$B \sin L\mu \left\{ p - pq^2 - \frac{(1+p^2)(1-q^2)}{1+pq} \right\} = 0 \qquad \text{(B-22)}$$

For a nontrivial solution it is necessary to have $\sin L\mu = 0$ which gives

$$\frac{A}{B} = \frac{\sin \mu}{q - \cos \mu} \qquad \text{(B-23)}$$

Any value of μ which satisfies the condition $\sin L\mu = 0$ can be used. Later considerations of the frequency spectra show that a convenient form is

$$\mu_m = \pi\left(1 + \frac{m-1}{L}\right) \qquad \text{(B-24)}$$

$$\gamma_m = \gamma(\mu_m) \qquad \text{(B-25)}$$

where $m = 1,2,3 \ldots$, and γ_m is the solution of (B-18) corresponding to μ_m. Now μ_m satisfies $\sin L\mu_m = 0$ so from (B-8), (B-16), (B-17), and (B-23) the modes are

$$\Phi_{m,\bar{\ell}}(\theta) = \left(\frac{\sin \bar{\ell}\mu_m - q_m \sin (\bar{\ell}-1)\mu_m}{q_m - \cos \mu_m}\right) f_m(\theta)$$

$$+ \left(\frac{\sin (\bar{\ell}-1)\mu_m - q_m \sin \bar{\ell}\mu_m}{q_m - \cos \mu_m}\right) f_m(1-\theta) \qquad \text{(B-26)}$$

where

$$f_m(\theta) = \sin \gamma_m\theta - (\sin \gamma_m \sinh \gamma_m\theta)/\sinh \gamma_m \qquad \text{(B-27)}$$

$$q_m = q(\gamma_m) \qquad \text{(B-28)}$$

If μ_m is a multiple of π the terms $\sin \bar{\ell}\mu_m$ and $\sin (\bar{\ell}-1)\mu_m$ in (B-26) are zero. Equation (B-18) has two possible solutions for this case, namely

$$q = \cos \mu = \pm 1 \quad ; \quad p = \text{arbitrary}$$

$$p = \cos \mu = \pm 1 \quad ; \quad q = \text{arbitrary}$$

For the first solution, $q = \pm 1$, (B-26) is indeterminate. However, it was pointed out earlier that for $q = \pm 1$ the modes are identical with those of a single span of length a. It follows from (B-18), (B-24), and (B-9) through (B-12) that the cases $m = 1, 2L+1, 4L+1 \ldots$, correspond to $q = -1$ so that from (B-15)

$$\Phi_{m,\bar{\ell}}(\theta) = (-1)^{\bar{\ell}-1}\left[f_m(\theta) + f_m(1-\theta)\right] \tag{B-29}$$

and if $m = L+1, 3L+1, 5L+1 \ldots$, $q = 1$ so that

$$\Phi_{m,\bar{\ell}}(\theta) = f_m(\theta) - f_m(1-\theta) \tag{B-30}$$

For the second solution of (B-18), i.e., $p = \pm 1$, (B-26) is degenerate and this solution is discarded.

The free vibration frequencies follow from the γ_m which in turn are determined by (B-18) and (B-24). The permissible values of γ and μ are illustrated in Fig. 5 for $\varepsilon = 0$ and 10. The smallest admissible value of γ is obtained for $\cos \mu = -1$, corresponding to the smallest γ obtained from (B-18) and (B-24) with $m = 1$. Setting $m = 2,3 \ldots L$ yields successively increasing values of γ, with $\gamma_L < 1.5056\,\pi$ (the lowest frequency of a clamped-clamped beam). Setting $m = L+1$ gives $\gamma = 1.5056\,\pi$ but this corresponds to the solution $p = 1$ of (B-18) which is degenerate. This solution is therefore discarded as trivial. The value $m = L+1$ gives a second value $\gamma > 1.5056\,\pi$ which is a permissible value, corresponding to the solution $q = 1$ of (B-18). Successively increasing values of γ are obtained by setting $m = L+2, L+3, \ldots 2L$. Setting $m = 2L+1$ yields a trivial solution $\gamma = 2.4998\,\pi$ corresponding to $p = -1$ and a permissible solution $\gamma > 2.4998\,\pi$.

Additional frequencies are obtained as indicated, with the trivial or degenerate solutions being successively the ascending frequencies of a clamped-clamped beam.

Figure 5 shows that the natural frequencies for the beam are contained within discrete frequency bands. These bands are independent of the number of bays, L , and the width of the bands decreases with increasing ϵ , i.e., as the clamped condition is approached. For a beam of L bays there are L discrete natural frequencies in each frequency band. Thus, for an infinitely extending beam the natural frequencies form a continuous spectrum throughout each band.

Table I (Appendix A) gives some insight into the physical significance of ϵ . In the table the first four frequencies for a one bay beam (L = 1) with ϵ = 0, 10, 100, and 1,000 are compared respectively to the first four frequencies for a clamped-clamped beam ($\epsilon = \infty$) . It is seen that, frequency-wise, ϵ = 10 lies approximately midway between the pinned case (ϵ = 0) and the clamped case, whereas ϵ = 1,000 very closely approximates the clamped condition.

To summarize, the chordwise deflection functions used in the flutter analysis are as follows:*

$$\bar{\Phi}_{m,\bar{\ell}}(\theta) = C_{m,\bar{\ell}} f_m(\theta) + D_{m,\bar{\ell}} f_m(1-\theta) \tag{B-31}$$

where

$$C_{m,\bar{\ell}} = \sin \bar{\ell}\mu_m - q_m \sin (\bar{\ell}-1)\mu_m$$

$$D_{m,\bar{\ell}} = \sin (\bar{\ell}-1)\mu_m - q_m \sin \bar{\ell}\mu_m \tag{B-32}$$

$$f_m(\theta) = \sin \gamma_m\theta - (\sin \gamma_m \sinh \gamma_m\theta)/\sinh \gamma_m \tag{B-33}$$

$$q_m = q(\gamma_m) \tag{B-34}$$

* The multiplying factor $\left(\frac{1}{q_m - \cos \mu_m}\right)$ in (B-26) is discarded.

with the special cases

$$C_{m,\bar{\ell}} = D_{m,\bar{\ell}} = (-1)^{\bar{\ell}-1} \tag{B-35}$$

for $m = 1, 2L+1, 4L+1, \ldots\ldots$

and

$$C_{m,\bar{\ell}} = 1$$

$$D_{m,\bar{\ell}} = -1 \tag{B-36}$$

for $m = L+1, 3L+1, 5L+1, \ldots\ldots$

In all cases frequencies are obtained as described earlier, taking $\epsilon = \epsilon_x$.

The spanwise deflection function $\psi_n(y)$ is not formulated here since it can be deduced from the formulations for $\Phi_m(x)$ by straightforward manipulation of the notation, taking $\epsilon = \epsilon_y$.

APPENDIX C

EVALUATION OF THE AERODYNAMIC INTEGRAL $I_{\bar{m},m,u}$

From Eqs. (22) and (28) of the report

$$I_{\bar{m},m,u} = \int_o^L \int_o^x P_u(\xi)\bar{\phi}_m(x-\xi)\Phi_{\bar{m}}(x)\, d\xi\, dx$$

where

$$P_u(\xi) = e^{-jKM\xi}\left\{-\left[(\Gamma_u{}^2/2) + (k^2/\beta^4)\right]J_o(\Gamma_u\xi) + (\Gamma_u{}^2/2)J_2(\Gamma_u\xi) + j(2k\Gamma_u/\beta^2)J_1(\Gamma_u\xi)\right\}$$

$$K = kM/\beta^2 \quad ; \quad \Gamma_u{}^2 = K^2 + (u\pi s/B\beta)^2 \quad \beta^2 = M^2-1 \quad j^2 = -1$$

Two procedures for evaluating $I_{\bar{m},m,u}$ are outlined in the report. The purpose of this Appendix is to present these procedures in detail.

Procedure 1

This procedure, the more approximate of the two, makes use of two basic approximations. First, the Bessel functions in $P_u(\xi)$ are approximated by sums of circular functions [3] .

$$J_o(\Gamma_u\xi) = \frac{1}{q}\sum_{r=1}^{q} \cos(\lambda_r\xi) + 2J_{4q}(\Gamma_u\xi)$$

$$J_1(\Gamma_u\xi) = \frac{1}{q}\sum_{r=1}^{q}\left[\cos\left(\frac{2r-1}{4q}\right)\pi\right]\sin(\lambda_r\xi) \qquad \text{(C-1)}$$

$$+\left[-J_{4q-1}(\Gamma_u\xi) + J_{4q+1}(\Gamma_u\xi)\right]$$

where

$$\lambda_r = \Gamma_u \cos\left(\frac{2r-1}{4q}\right)\pi \tag{C-2}$$

The term(s) appearing outside of the summation sign give an estimate of the error in the representation and consequently are omitted in the analysis. In the numerical work, $J_2(\Gamma_u\xi)$ is replaced by means of the identity

$$J_2(\Gamma_u\xi) = \frac{2J_1(\Gamma_u\xi)}{\Gamma_u\xi} - J_o(\Gamma_u\xi)$$

The second basic approximation introduced in this procedure is the expansion of the chordwise deflection function, Φ_m , in a truncated sine series

$$\Phi_m(x) = \sum_t A_{m,t} \sin\frac{t\pi x}{L} \tag{C-3}$$

Substitution of these approximations gives

$$I_{\bar{m},m,u} = L^2 \sum_t \sum_{\bar{t}} A_{m,t} A_{\bar{m},\bar{t}} Z_{t,\bar{t},u} \tag{C-4}$$

where

$$Z_{t,\bar{t},u} = \frac{j}{2} E_t \delta_{t,\bar{t}} + \frac{1}{L}\left\{-F_t \bar{\epsilon}_{t,\bar{t}} - (-1)^{\bar{t}} L_e^{-jKML} G_{t,\bar{t}} + H_{t,\bar{t}}\right\} \tag{C-5}$$

$$\begin{aligned} \delta_{t,\bar{t}} &= 0 \text{ if } t \neq \bar{t} \\ &= 1 \text{ if } t = \bar{t} \end{aligned} \tag{C-6}$$

$$\epsilon_{t,t} = 0 \text{ if } (t+\bar{t})L \text{ is even}$$

$$= \frac{2\bar{t}}{\pi(t^2-\bar{t}^2)} \text{ if } (t+\bar{t})L \text{ is odd} \tag{C-7}$$

$$k = \frac{\omega a}{U} \tag{C-8}$$

$$s = \frac{a}{b} \tag{C-9}$$

$$\lambda_r = \Gamma_u \cos\left(\frac{2r-1}{4q}\right)\pi \tag{C-10}$$

$$a_r = -\frac{L^2}{q}\left[(KM-k)^2 + \lambda_r^2\right] \tag{C-11}$$

$$b_r = \frac{2kL^2}{q\beta^2}\lambda_r \tag{C-12}$$

$$c_{r,t} = \frac{KM}{2L}\left[\frac{1}{\left[\lambda_r+t\pi/L\right]^2 - (KM)^2} - \frac{1}{\left[\lambda_r-t\pi/L\right]^2 - (KM)^2}\right] \tag{C-13}$$

$$d_{r,t} = \frac{KM}{2L}\left[\frac{1}{\left[\lambda_r+t\pi/L\right]^2 - (KM)^2} + \frac{1}{\left[\lambda_r-t\pi/L\right]^2 - (KM)^2}\right] \tag{C-14}$$

$$e_{r,t} = \frac{1}{2L}\left[\frac{\lambda_r+t\pi/L}{\left[\lambda_r+t\pi/L\right]^2 - (KM)^2} - \frac{\lambda_r-t\pi/L}{\left[\lambda_r-t\pi/L\right]^2 - (KM)^2}\right] \tag{C-15}$$

$$f_{r,t} = \frac{1}{2L}\left[\frac{\lambda_r + t\pi/L}{[\lambda_r + t\pi/L]^2 - (KM)^2} + \frac{\lambda_r - t\pi/L}{[\lambda_r - t\pi/L]^2 - (KM)^2}\right] \qquad (C\text{-}16)$$

$$g_{r,t,\bar{t}} = e_{r,t}e_{r,\bar{t}} + c_{r,t}c_{r,\bar{t}} \qquad (C\text{-}17)$$

$$h_{r,t,\bar{t}} = e_{r,t}c_{r,\bar{t}} + e_{r,\bar{t}}c_{r,t} \qquad (C\text{-}18)$$

$$E_t = \sum_{r=1}^{q} (a_r d_{r,t} + b_r f_{r,t}) \qquad (C\text{-}19)$$

$$F_t = \sum_{r=1}^{q} (a_r e_{r,t} + b_r c_{r,t}) \qquad (C\text{-}20)$$

$$G_{t,\bar{t}} = \sum_{r=1}^{q} \left[(a_r g_{r,t,\bar{t}} + b_r h_{r,t,\bar{t}}) \cos \lambda_r L + j(a_r h_{r,t,\bar{t}} + b_r g_{r,t,\bar{t}}) \sin \lambda_r L\right] \qquad (C\text{-}21)$$

$$H_{t,\bar{t}} = \sum_{r=1}^{q} \left[a_r g_{r,t,\bar{t}} + b_r h_{r,t,\bar{t}}\right] \qquad (C\text{-}22)$$

Procedure 1, just outlined, is suitable only for small values of m, L, and the argument of the Bessel functions $\Gamma_u\xi$. For large values of these parameters the number of terms that must be carried in the series approximations becomes prohibitive. Roughly speaking the procedure is practical for $m \leq 4$, $L \leq 2$, and $\Gamma_u\xi \leq 10$.

Procedure 2

When the first procedure is not practical it is best to approach the integral $I_{\bar{m},m,u}$ by first changing the order of integration to give

$$I_{\bar{m},m,u} = \int_0^L P_u(\xi) \int_\xi^L \Phi_m(x-\xi)\Phi_{\bar{m}}(x)\, dx\, d\xi \qquad (C\text{-}23)$$

If local coordinates

$$\theta = x - (\bar{\ell}-1) \quad ; \quad \bar{\ell}-1 \le x \le \bar{\ell} \qquad (C\text{-}24)$$

$$\varphi = \xi - (\ell-1) \quad ; \quad \ell-1 \le \xi \le \ell \qquad (C\text{-}25)$$

are introduced (C-23) becomes

$$I_{\bar{m},m,u} = \sum_{\ell=1}^{L} \sum_{\bar{\ell}=\ell}^{L} \int_0^1 P_u(\ell-1+\varphi) \int_\varphi^1 \Phi_{m,\bar{\ell}-\ell+1}(\theta-\varphi)\Phi_{\bar{m},\bar{\ell}}(\theta)\, d\theta\, d\varphi$$

$$+ \sum_{\ell=1}^{L-1} \sum_{\bar{\ell}=\ell+1}^{L} \int_0^1 P_u(\ell-1+\varphi) \int_0^\varphi \Phi_{m,\bar{\ell}-\ell}(1+\theta-\varphi)\Phi_{\bar{m},\bar{\ell}}(\theta)\, d\theta\, d\varphi \qquad (C\text{-}26)$$

From the definition of the chordwise deflection function given in Appendix B, it is clear that

$$\Phi_{m,\ell}(\theta) = C_{m,\ell} f_m(\theta) + D_{m,\ell} f_m(1-\theta)$$

$$\Phi_{m,\bar{\ell}-\ell+1}(\theta-\varphi) = C_{m,\bar{\ell}-\ell+1} f_m(\theta-\varphi) + D_{m,\bar{\ell}-\ell+1} f_m(1-\theta+\varphi)$$

$$\Phi_{m,\bar{\ell}-\ell}(1+\theta-\varphi) = C_{m,\bar{\ell}-\ell} f_m(1+\theta-\varphi) + D_{m,\bar{\ell}-\ell} f_m(\varphi-\theta)$$

where

$$f_m(v) = \sin \gamma_m v - \frac{\sin \gamma_m}{\sinh \gamma_m} \sinh \gamma_m v$$

It is therefore convenient to introduce the following general integral definitions

$$\int_a^b f_m^{(\alpha\theta)}(\theta-p) f_{\bar{m}}(\theta)\, d\theta = F_{\bar{m},m}(\theta-p,\theta,\alpha)\Big|_a^b$$

$$= F_{\bar{m},m}(b-p,b,\alpha) - F_{\bar{m},m}(a-p,a,\alpha) \qquad \text{(C-27)}$$

where from [5]

$$F_{\bar{m},m}(\theta-p,\theta,\alpha) = \frac{1}{4}\theta f_m^{(\alpha\theta)}(\theta-p) f_{\bar{m}}(\theta)$$

$m = \bar{m}$

$$- \frac{\theta}{4\gamma_{\bar{m}}^4}\left\{f_{\bar{m}}^{[(\alpha+1)\theta]}(\theta-p) f_{\bar{m}}^{(3\theta)}(\theta) + f_{\bar{m}}^{[(\alpha+3)\theta]}(\theta-p) f_{\bar{m}}^{(\theta)}(\theta)\right\}$$

$$- \frac{1}{8\gamma_{\bar{m}}^4}\left\{f_{\bar{m}}^{[(\alpha+2)\theta]}(\theta-p) f_{\bar{m}}^{(\theta)}(\theta) + f_{\bar{m}}^{[(\alpha+1)\theta]}(\theta-p) f_{\bar{m}}^{(2\theta)}(\theta)\right\}$$

$$+ \frac{\theta}{4\gamma_{\bar{m}}^4} f_{\bar{m}}^{[(\alpha+2)\theta]}(\theta-p) f_{\bar{m}}^{(2\theta)}(\theta)$$

$$+ \frac{3}{8\gamma_{\bar{m}}^4}\left\{f_{\bar{m}}^{(\alpha\theta)}(\theta-p) f_{\bar{m}}^{(3\theta)}(\theta) + f_{\bar{m}}^{[(\alpha+3)\theta]}(\theta-p) f_{\bar{m}}(\theta)\right\} \qquad \text{(C-28)}$$

and

$$F_{\bar{m},m}(\theta-p,\theta,\alpha) = \frac{1}{\gamma_m^4-\gamma_{\bar{m}}^4}\left\{f_m^{[(\alpha+3)\theta]}(\theta-p)f_{\bar{m}}(\theta) - f_m^{(\alpha\theta)}(\theta-p)f_{\bar{m}}^{(3\theta)}(\theta)\right.$$

$m \neq \bar{m}$

$$\left. + f_m^{[(\alpha+1)\theta]}(\theta-p)f_{\bar{m}}^{(2\theta)}(\theta) - f_m^{[(\alpha+2)\theta]}(\theta-p)f_{\bar{m}}^{(\theta)}(\theta)\right\} \quad (C\text{-}29)$$

In these definitions, $f_m^{(\alpha\theta)}(\theta)$ for $\alpha = 0$ is $f_m(\theta)$, and not unity as the notation seems to suggest. Using the definitions (C-27) to (C-29) the aerodynamic integral becomes

$$I_{\bar{m},m,u} = \sum_{\ell=1}^{L}\int_o^1 P_u(\ell-1+\varphi)G_{\bar{m},m,\ell}(\varphi)\,d\varphi$$

$$+ \sum_{\ell=1}^{L-1}\int_o^1 P_u(\ell-1+\varphi)H_{\bar{m},m,\ell}(\varphi)\,d\varphi \quad (C\text{-}30)$$

where

$$G_{\bar{m},m,\ell} = \sum_{\bar{\ell}=\ell}^{L}\int_\varphi^1 \Phi_{m,\bar{\ell}-\ell+1}(\theta-\varphi)\Phi_{\bar{m},\bar{\ell}}(\theta)\,d\theta$$

$$= \left\{F_{\bar{m},m}(1-\varphi,1,0) - F_{\bar{m},m}(0,\varphi,0)\right\}\sum_{\bar{\ell}=\ell}^{L} C_{m,\bar{\ell}-\ell+1}C_{\bar{m},\bar{\ell}}$$

$$- \left\{F_{\bar{m},m}(0,1-\varphi,0) - F_{\bar{m},m}(\varphi-1,0,0)\right\}\sum_{\bar{\ell}=\ell}^{L} C_{m,\bar{\ell}-\ell+1}D_{\bar{m},\bar{\ell}}$$

$$- \left\{F_{\bar{m},m}(-\varphi,1,0) - F_{\bar{m},m}(-1,\varphi,0)\right\}\sum_{\bar{\ell}=\ell}^{L} D_{m,\bar{\ell}-\ell+1}C_{\bar{m},\bar{\ell}}$$

$$+ \left\{F_{\bar{m},m}(1,1-\varphi,0) - F_{\bar{m},m}(\varphi,0,0)\right\}\sum_{\bar{\ell}=\ell}^{L} D_{m,\bar{\ell}-\ell+1}D_{\bar{m},\bar{\ell}} \quad (C\text{-}31)$$

$$H_{\bar{m},m,\ell} = \sum_{\bar{\ell}=\ell+1}^{L} \int_{o}^{\varphi} \Phi_{m,\bar{\ell}-\ell}(1+\theta-\varphi)\delta_{\bar{m},\bar{\ell}}(\theta)\, d\theta$$

$$= \left\{ F_{\bar{m},m}(1,\varphi,0) - F_{\bar{m},m}(1-\varphi,0,0) \right\} \sum_{\bar{\ell}=\ell+1}^{L} C_{m,\bar{\ell}-\ell} C_{\bar{m},\bar{\ell}}$$

$$- \left\{ F_{\bar{m},m}(\varphi-1,1,0) - F_{\bar{m},m}(-1,1-\varphi,0) \right\} \sum_{\bar{\ell}=\ell+1}^{L} C_{m,\bar{\ell}-\ell} D_{\bar{m},\bar{\ell}}$$

$$- \left\{ F_{\bar{m},m}(0,\varphi,0) - F_{\bar{m},m}(-\varphi,0,0) \right\} \sum_{\bar{\ell}=\ell+1}^{L} D_{m,\bar{\ell}-\ell} C_{\bar{m},\bar{\ell}}$$

$$+ \left\{ F_{\bar{m},m}(\varphi,1,0) - F_{\bar{m},m}(0,1-\varphi,0) \right\} \sum_{\bar{\ell}=\ell+1}^{L} D_{m,\bar{\ell}-\ell} D_{\bar{m},\bar{\ell}} \qquad \text{(C-32)}$$

The integrals $\int_{o}^{1} P_u(\ell-1+\varphi) G_{\bar{m},m,\ell}(\varphi)\, d\varphi$ and $\int_{o}^{1} P_u(\ell-1+\varphi) H_{\bar{m},m,\ell}(\varphi)\, d\varphi$ in (C-30) are evaluated numerically.

APPENDIX D

EVALUATION OF INTEGRALS $J_{\bar{m},m}, K_{\bar{m},m}, R_{\bar{m},m}$, S, T, Q

The integrals $J_{\bar{m},m}$, $K_{\bar{m},m}$, and $R_{\bar{m},m}$ involve the chordwise deflection functions Φ_m and their derivatives. Therefore introduce local coordinates and deflections from Appendix B,

$$\theta = \frac{x}{a} - (\ell-1) \qquad (\ell-1)a \le x \le \ell a \tag{D-1}$$

$$\Phi_m = \Phi_{m,\ell} \qquad \ell = 1,2,3, \ldots\ldots L \tag{D-2}$$

The integrals can then be written as

$$J_{\bar{m},m} = \int_o^L \Phi_m(x)\Phi_{\bar{m}}(x)\,dx = \sum_{\ell=1}^{L} \int_o^1 \Phi_{m,\ell}(\theta)\Phi_{\bar{m},\ell}(\theta)\,d\theta \tag{D-3}$$

$$K_{\bar{m},m} = \int_o^L \Phi_m^{(2x)}(x)\Phi_{\bar{m}}(x)\,dx = \sum_{\ell=1}^{L} \int_o^1 \Phi_{m,\ell}^{(2\theta)}(\theta)\Phi_{\bar{m},\ell}(\theta)\,d\theta) \tag{D-4}$$

$$R_{\bar{m},m} = \int_o^L \Phi_m^{(x)}(x)\Phi_{\bar{m}}(x)\,dx = \sum_{\ell=1}^{L} \int_o^1 \Phi_{m,\ell}^{(\theta)}(\theta)\Phi_{\bar{m},\ell}(\theta)\,d\theta \tag{D-5}$$

These integrals can be evaluated conveniently by referring to the $F_{\bar{m},m}$ functions introduced in Appendix C, Eqs. (C-28) and (C-29). There results

$$J_{\bar{m},m} = \left\{ F_{\bar{m},m}(1,1,0) - F_{\bar{m},m}(0,0,0) \right\} \sum_{\ell=1}^{L} \left(C_{m,\ell}C_{\bar{m},\ell} + D_{m,\ell}D_{\bar{m},\ell} \right)$$

$$+ \left\{ F_{\bar{m},m}(0,-1,0) - F_{\bar{m},m}(1,C,0) \right\} \sum_{\ell=1}^{L} \left(C_{m,\ell}D_{\bar{m},\ell} + D_{m,\ell}C_{\bar{m},\ell} \right) \tag{D-6}$$

$$K_{\bar{m},m} = \left\{ F_{\bar{m},m}(1,1,2) - F_{\bar{m},m}(0,0,2) \right\} \sum_{\ell=1}^{L} (C_{m,\ell} C_{\bar{m},\ell} + D_{m,\ell} D_{\bar{m},\ell})$$

$$+ \left\{ F_{\bar{m},m}(0,-1,2) - F_{\bar{m},m}(1,0,2) \right\} \sum_{\ell=1}^{L} (C_{m,\ell} D_{\bar{m},\ell} + D_{m,\ell} C_{\bar{m},\ell}) \qquad \text{(D-7)}$$

$$R_{\bar{m},m} = \left\{ F_{\bar{m},m}(1,1,1) - F_{\bar{m},m}(0,0,1) \right\} \sum_{\ell=1}^{L} (C_{m,\ell} C_{\bar{m},\ell} - D_{m,\ell} D_{\bar{m},\ell})$$

$$+ \left\{ F_{\bar{m},m}(0,-1,1) - F_{\bar{m},m}(1,0,1) \right\} \sum_{\ell=1}^{L} (C_{m,\ell} D_{\bar{m},\ell} - D_{m,\ell} C_{\bar{m},\ell}) \qquad \text{(D-8)}$$

The integrals S, T, and Q involve the spanwise deflection shape ψ_n and its derivatives. Introduce local coordinates and deflection

$$\eta = y - (k-1) \qquad k-1 \le y \le k \qquad \text{(D-9)}$$

$$\psi_n = \psi_{n,k} \qquad k = 1,2,3, \ldots\ldots N \qquad \text{(D-10)}$$

and subsequently obtain

$$S = \int_o^N \psi_n^2 \, dy = \sum_{k=1}^{N} \int_o^1 \psi_{n,k}^2(\eta) \, d\eta \qquad \text{(D-11)}$$

$$T = \int_o^N \psi_n^{(2y)} \psi_n \, dy = \sum_{k=1}^{N} \int_o^1 \psi_{n,k}^{(2\eta)}(\eta) \psi_{n,k}(\eta) \, d\eta \qquad \text{(D-12)}$$

$$Q = \int_o^N \psi_n^{(4y)} \psi_n \, dy = \sum_{k=1}^{N} \int_o^1 \psi_{n,k}^{(4\eta)}(\eta) \psi_{n,k}(\eta) \, d\eta \qquad \text{(D-13)}$$

Since these integrals depend on the spanwise deflection shape, it is again necessary to consider each of the five physical situations of interest to the present analysis. These situations are listed in detail in the report body and in Appendix E. It turns out that for cases 1, 2, and 3

$$S = \sum_{k=1}^{N} \frac{1}{4\bar{\gamma}_n^4} \left\{ -2\left[\bar{C}_{n,k}\bar{f}_n^{(\eta)}(1) - \bar{D}_{n,k}\bar{f}_n^{(\eta)}(0)\right] \times \left[\bar{C}_{n,k}\bar{f}_n^{(3\eta)}(1) - \bar{D}_{n,k}\bar{f}_n^{(3\eta)}(0)\right] + \left[\bar{C}_{n,k}\bar{f}_n^{(2\eta)}(1) + \bar{D}_{n,k}\bar{f}_n^{(2\eta)}(0)\right]^2 - \left[\bar{C}_{n,k}\bar{f}_n^{(\eta)}(1) - \bar{D}_{n,k}\bar{f}_n^{(\eta)}(0)\right]\left[\bar{C}_{n,k}\bar{f}_n^{(2\eta)}(1) + \bar{D}_{n,k}\bar{f}_n^{(2\eta)}(0)\right] + \left[\bar{C}_{n,k}\bar{f}_n^{(\eta)}(0) - \bar{D}_{n,k}\bar{f}_n^{(\eta)}(1)\right]\left[\bar{C}_{n,k}\bar{f}_n^{(2\eta)}(0) + \bar{D}_{n,k}\bar{f}_n^{(2\eta)}(1)\right] \right\} \quad \text{(D-16)}$$

$$T = \sum_{k=1}^{N} \frac{1}{4\bar{\gamma}_n^4} \left\{ -\bar{\gamma}_n^4\left[\bar{C}_{n,k}\bar{f}_n^{(\eta)}(1) - \bar{D}_{n,k}\bar{f}_n^{(\eta)}(0)\right]^2 - \left[\bar{C}_{n,k}\bar{f}_n^{(3\eta)}(1) - \bar{D}_{n,k}\bar{f}_n^{(3\eta)}(0)\right]^2 + \left[\bar{C}_{n,k}\bar{f}_n^{(2\eta)}(1) + \bar{D}_{n,k}\bar{f}_n^{(2\eta)}(0)\right]\left[\bar{C}_{n,k}\bar{f}_n^{(3\eta)}(1) - \bar{D}_{n,k}\bar{f}_n^{(3\eta)}(0)\right] - \left[\bar{C}_{n,k}\bar{f}_n^{(2\eta)}(0) + \bar{D}_{n,k}\bar{f}_n^{(2\eta)}(1)\right]\left[\bar{C}_{n,k}\bar{f}_n^{(3\eta)}(0) - \bar{D}_{n,k}\bar{f}_n^{(3\eta)}(1)\right] \right\} \quad \text{(D-17)}$$

$$Q = \bar{\gamma}_n^4 S \quad \text{(D-18)}$$

For cases 4 and 5 these quantities reduce to simply

$$S = 1$$

$$T = Q = 0 \quad \text{(D-19)}$$

APPENDIX E

EVALUATION OF FOURIER COEFFICIENTS $B_{n,u}$ AND THE INTEGRAL $F(u)$

The spanwise deflection shape $\psi_n(y)$ is expanded in a sine series

$$\psi_n = \sum_u B_{n,u} \sin \frac{u\pi\phi}{B} \tag{E-1}$$

where ϕ is the transformed coordinate (Fig. 3)

$$\phi = y + \lambda$$

$$B = 2\lambda + N \tag{E-2}$$

and λ is a constant to be evaluated. The coefficients $B_{n,u}$ are given by

$$B_{n,u} = \frac{2}{B}\int_o^B \psi_n(\phi) \sin \frac{u\pi\phi}{B}\, d\phi \tag{E-3}$$

These coefficients are to be evaluated for each of the five physical situations to be analyzed. The situations are repeated here for completeness.

(1) A panel array as shown in Fig. 1 with a finite number of panels in both the chordwise and spanwise direction. The array is bordered by an inflexible surface extending to infinity in all directions.

(2) The same as (1) except that the array extends to infinity in the spanwise direction.

(3) The same as (1) except that the array is flanked on the sides by vertical walls (a wind tunnel installation for instance) an arbitrary distance from the edge of the array.

(4) The same as (1) except that the array has one panel in the spanwise direction (N=1) and the side edges are free.

(5) The same as (4) except that the array is flanked by vertical walls as described in (3).

Before evaluating the $B_{n,u}$ it is useful to first determine λ for each case. Geometrical aspects of the expansion (E-1) are shown in Fig. 3 for cases (1) and (4). The finite span deflection shape is depicted in Fig. 3a, and the periodic expansion of $\psi_n\omega$ shown in Fig. 3b. The domain of aerodynamic influence is illustrated in Fig. 3c. All points inside the shaded region are aerodynamically coupled to the panel configuration being analyzed. It is seen that for $\lambda \geq sL/2M$ the periodic reflections of ψ_n are outside the coupled region and the effect of an isolated panel array is obtained.

For cases (3) and (5) the effect of vertical walls is obtained by introducing fictitious image panels on each side of the real panel. The geometrical aspects of this situation are shown in Fig. 4. The wall locations must be planes of symmetry in the flow and this situation is realized when

$$\frac{sL}{M} \leq N+2A$$

The desired aerodynamic isolation is obtained by taking $\lambda = N+3A/2$.

The case of a panel array extending to infinity in the spanwise direction (case 2) offers some difficulty. In accordance with the discussion in the report body, ψ_n is restricted to cases in which the deflection in adjacent panels is antisymmetric in which case $\lambda = 0$ and $B = 1$.

In summary, then, λ is taken as follows.

Case	λ
1	$sL/2M$
2	0
3	larger of $sL/2M$ and $N+3A/2$
4	$sL/2M$
5	larger of $sL/2M$ and $N+3A/2$

The coefficients $B_{n,u}$ are evaluated in the following sections.

Case 1 - Panel Array of Finite Spanwise Extent

The deflection is given by

$$\begin{aligned} \psi_n &= 0 && 0 \le \phi \le \lambda \\ \psi_n &= \psi_n && \lambda \le \phi \le \lambda+N \\ \psi_n &= 0 && \lambda+N \le \phi \le 2\lambda+N \end{aligned} \qquad \text{(E-4)}$$

From (E-3) there follows

$$B_{n,u} = \frac{2}{B} \int_{\lambda}^{\lambda+N} \psi_n(\phi) \sin \frac{u\pi\phi}{B} \, d\phi \qquad \text{(E-5)}$$

Introducing local coordinates and a local deflection

$$\begin{aligned} \eta &= y-(k-1) \quad ; \quad k-1 \le y \le k \\ \psi_n &= \psi_{n,k}(\eta) \quad ; \quad k = 1,2 \ldots N \end{aligned} \qquad \text{(E-6)}$$

yields

$$B_{n,u} = \frac{2B^3}{B^4\bar{\gamma}_n^4 - u^4\pi^4} \sum_{k=1}^{N} \left\{ \left\{ \bar{C}_{n,k}\bar{f}_n^{(3\eta)}(1) - \bar{D}_{n,k}\bar{f}_n^{(3\eta)}(0) \right.\right.$$

$$\left. - \left(\frac{u\pi}{B}\right)^2 \left[\bar{C}_{n,k}\bar{f}_n^{(\eta)}(1) - \bar{D}_{n,k}\bar{f}_n^{(\eta)}(0)\right] \right\} \sin \frac{u\pi}{B}(k+\lambda)$$

$$- \left(\frac{u\pi}{B}\right) \left[\bar{C}_{n,k}\bar{f}_n^{(2\eta)}(1) + \bar{D}_{n,k}\bar{f}_n^{(2\eta)}(0)\right] \cos \frac{u\pi}{B}(k+\lambda) - \left\{ \bar{C}_{n,k}\bar{f}_n^{(3\eta)}(0) \right.$$

$$\left. - \bar{D}_{n,k}\bar{f}_n^{(3\eta)}(1) - \left(\frac{u\pi}{B}\right)^2 \left[\bar{C}_{n,k}\bar{f}_n^{(\eta)}(0) - \bar{D}_{n,k}\bar{f}_n^{(\eta)}(1)\right] \right\} \sin \frac{u\pi}{B}(k+\lambda-1)$$

$$\left. + \left(\frac{u\pi}{B}\right) \left[\bar{C}_{n,k}\bar{f}_n^{(2\eta)}(0) + \bar{D}_{n,k}\bar{f}_n^{(2\eta)}(1)\right] \cos \frac{u\pi}{B}(k+\lambda-1) \right\} \qquad \text{(E-7)}$$

where $\bar{C}_{n,k}$, $\bar{D}_{n,k}$ and $\bar{f}_n(\eta)$ are defined in Appendix B .

Case 2 - Panel Array of Infinite Spanwise Extent

The coefficients for this case are obtained from (E-7) by setting $k = N = B = 1$. There follows

$$B_{n,u} = \frac{2u\pi}{\bar{\gamma}_n^4 - (u\pi)^4} \left\{ \bar{C}_{n,1}\bar{f}_n^{(2\eta)}(0) + \bar{D}_{n,1}\bar{f}_n^{(2\eta)}(1) \right.$$

$$\left. - (-1)^u \left[\bar{C}_{n,1}\bar{f}_n^{(2\eta)}(1) + \bar{D}_{n,1}\bar{f}_n^{(2\eta)}(0)\right] \right\} \qquad \text{(E-8)}$$

Case 3 - Panel Array of Finite Spanwise Extent with Vertical Side Walls

The deflection is given by (Fig. 4)

$$\begin{aligned}
\psi_n &= 0 && 0 \le \phi \le \lambda-N-A \\
\psi_n &= \psi_n && \lambda-N-A \le \phi \le \lambda-A \\
\psi_n &= 0 && \lambda-A \le \phi \le \lambda \\
\psi_n &= \psi_n && \lambda \le \phi \le \lambda+N \\
\psi_n &= 0 && \lambda+N \le \phi \le \lambda+N+A \\
\psi_n &= \psi_n && \lambda+N+A \le \phi \le \lambda+2N+A \\
\psi_n &= 0 && \lambda+2N+A \le \phi \le 2\lambda+N
\end{aligned} \tag{E-9}$$

From (E-3) there follows

$$B_{n,u} = \frac{2}{B} \int_{\lambda-N-A}^{\lambda-A} \psi_n(\phi) \sin \frac{u\pi\phi}{B} \, d\phi + \frac{2}{B} \int_{\lambda}^{\lambda+N} \psi_n(\phi) \sin \frac{u\pi\phi}{B} \, d\phi$$

$$+ \frac{2}{B} \int_{\lambda+N+A}^{\lambda+2N+A} \psi_n(\phi) \sin \frac{u\pi\phi}{B} \, d\phi \tag{E-10}$$

which gives

$$B_{n,u} = \frac{2B^3}{B^4\bar{\gamma}_n^4 - u^4\pi^4} \sum_{k=1}^{N} \left\{ \left[\bar{C}_{n,k} \bar{f}_n^{(3\eta)}(1) - \bar{D}_{n,k} \bar{f}_n^{(3\eta)}(0) \right.\right.$$

$$\left. - \left(\frac{u\pi}{B}\right)^2 \left[\bar{C}_{n,k} \bar{f}_n^{(\eta)}(1) - \bar{D}_{n,k} \bar{f}_n^{(\eta)}(0) \right] \right] \left[\sin \frac{u\pi}{B} (k+\lambda-N-A) + \sin \frac{u\pi}{B} (k+\lambda) \right.$$

$$\left. + \sin \frac{u\pi}{B} (k+\lambda+A+N) \right]$$

$$- \frac{u\pi}{B} \left[\bar{C}_{n,k} \bar{f}_n^{(2\eta)}(1) + \bar{D}_{n,k} \bar{f}_n^{(2\eta)}(0) \right] \left[\cos \frac{u\pi}{B} (k+\lambda-N-A) + \cos \frac{u\pi}{B} (k+\lambda) \right.$$

$$\left. + \cos \frac{u\pi}{B} (k+\lambda+A+N) \right]$$

$$- \left[\bar{C}_{n,k} \bar{f}_n^{(3\eta)}(0) - \bar{D}_{n,k} \bar{f}_n^{(3\eta)}(1) - \frac{u\pi}{B} \left[\bar{C}_{n,k} \bar{f}_n^{(\eta)}(0) - \bar{D}_{n,k} \bar{f}_n^{(\eta)}(1) \right] \right]$$

$$\times \left[\sin \frac{u\pi}{B} (k-1+\lambda-N-A) + \sin \frac{u\pi}{B} (k-1+\lambda) + \sin \frac{u\pi}{B} (k-1+\lambda+A+N) \right]$$

$$+ \frac{u\pi}{B} \left[\bar{C}_{n,k} \bar{f}_n^{(2\eta)}(0) + \bar{D}_{n,k} \bar{f}_n^{(2\eta)}(1) \right]$$

$$\left. \times \left[\cos \frac{u\pi}{B} (k-1+\lambda-N-A) + \cos \frac{u\pi}{B} (k-1+\lambda) + \cos \frac{u\pi}{B} (k-1+\lambda+A+N) \right] \right\} \qquad \text{(E-11)}$$

Case 4 - Panel Array with N = 1 and Side Edges Free

The deflection is given by

$$\psi_n = 0 \qquad 0 \le \phi \le \lambda$$

$$\psi_n = 1 \qquad \lambda \le \phi \le \lambda+1$$

$$\psi_n = 0 \qquad \lambda+1 \le \phi \le 2\lambda+1 \qquad \text{(E-12)}$$

From (E-3) there follows

$$B_{n,u} = \frac{2}{B} \int_o^1 \sin \frac{u\pi}{B} (\phi+\lambda)\, d\phi \tag{E-13}$$

or

$$B_{n,u} = \frac{2}{u\pi} \left[1-(-1)^u\right] \cos \frac{u\pi}{B} \lambda \tag{E-14}$$

Case 5 - Panel Array with $N = 1$, Side Edges Free and with Vertical Side Walls

This case is a special form of case 3 with $k = N = \psi_n = 1$. Straightforward integration gives

$$B_{n,u} = \frac{2}{u\pi} \left\{ \cos \frac{u\pi}{B} (\lambda-A-1) - \cos \frac{u\pi}{B} (\lambda-A) + \cos \frac{u\pi}{B} (\lambda) \right.$$

$$- \cos \frac{u\pi}{B} (\lambda+1) + \cos \frac{u\pi}{B} (\lambda+A+1)$$

$$\left. - \cos \frac{u\pi}{B} (\lambda+A+2) \right\} \tag{E-15}$$

A second purpose of this Appendix is to evaluate the integral

$$F(u) = \int_\lambda^{\lambda+N} \psi_n \sin \frac{u\pi\phi}{B}\, d\phi \tag{E-16}$$

introduced in Eq. (29) of the section dealing with the aerodynamic terms. In evaluating $F(u)$ it is again necessary to be cognizant of the five physical cases of interest. Comparison of (E-16) with (E-3) shows that for cases (1), (2), and (4)

$$F(u) = BB_{n,u}/2 \tag{E-17}$$

For cases (3) and (5), F(u) can be evaluated in closed form to give:

Case (3)

$$F(u) = \frac{B^4}{(B\tilde{\gamma}_n)^4-(u\pi)^4} \sum_{k=1}^{N} \left\{ \left[\bar{C}_{n,k} \bar{f}_n^{(3\eta)}(1) - \bar{D}_{n,k} \bar{f}_n^{(3\eta)}(0) \right.\right.$$

$$\left. - \left(\frac{u\pi}{B}\right)^2 \left[\bar{C}_{n,k} \bar{f}_n^{(\eta)}(1) - \bar{D}_{n,k} \bar{f}_n^{(\eta)}(0) \right] \right] \sin \frac{u\pi}{B} (k+\lambda)$$

$$+ \left[\left(\frac{u\pi}{B}\right)^2 \left[\bar{C}_{n,k} \bar{f}_n^{(\eta)}(0) - \bar{D}_{n,k} \bar{f}_n^{(\eta)}(1) \right] - \bar{C}_{n,k} \bar{f}_n^{(3\eta)}(0) \right.$$

$$\left. + \bar{D}_{n,k} \bar{f}_n^{(3\eta)}(1) \right] \sin \frac{u\pi}{B} (k-1+\lambda)$$

$$- \left[\frac{u\pi}{B} \left[\bar{C}_{n,k} \bar{f}_n^{(2\eta)}(1) + \bar{D}_{n,k} \bar{f}_n^{(2\eta)}(0) \right] \right] \cos \frac{u\pi}{B} (k+\lambda)$$

$$+ \left[\frac{u\pi}{B} \left[\bar{C}_{n,k} \bar{f}_n^{(2\eta)}(0) + \bar{D}_{n,k} \bar{f}_n^{(2\eta)}(1) \right] \right] \cos \frac{u\pi}{B} (k-1+\lambda) \Bigg\} \qquad \text{(E-18)}$$

Case (5)

$$F(u) = \frac{B}{u\pi} \left[\cos \frac{u\pi}{B} \lambda - \cos \frac{u\pi}{B} (\lambda+1) \right] \qquad \text{(E-19)}$$

NASA CR-80
National Aeronautics and Space Administration.
RESEARCH ON PANEL FLUTTER. D. R. Kobett,
Midwest Research Institute. July 1964. viii, 67p.
OTS price, $2.00.
(NASA CONTRACTOR REPORT CR-80)

A computer program was developed which is particularly well suited for use in parametric flutter investigations where a large quantity of numerical data is required. The underlying analysis used exact, linearized, three-dimensional aerodynamic theory so the program can be used to investigate the critical low supersonic regime. Finite panel arrays can be treated, and wind-tunnel installations can be simulated. A limited quantity of informative numerical data is presented. Most of the data pertains to the flutter of single panels with free side edges, with and without adjacent vertical side walls.

I. Kobett, D. R.
II. Midwest Research Institute
III. NASA CR-80

NASA

NASA CR-80
National Aeronautics and Space Administration.
RESEARCH ON PANEL FLUTTER. D. R. Kobett,
Midwest Research Institute. July 1964. viii, 67p.
OTS price, $2.00.
(NASA CONTRACTOR REPORT CR-80)

A computer program was developed which is particularly well suited for use in parametric flutter investigations where a large quantity of numerical data is required. The underlying analysis used exact, linearized, three-dimensional aerodynamic theory so the program can be used to investigate the critical low supersonic regime. Finite panel arrays can be treated, and wind-tunnel installations can be simulated. A limited quantity of informative numerical data is presented. Most of the data pertains to the flutter of single panels with free side edges, with and without adjacent vertical side walls.

I. Kobett, D. R.
II. Midwest Research Institute
III. NASA CR-80

NASA

NASA CR-80
National Aeronautics and Space Administration.
RESEARCH ON PANEL FLUTTER. D. R. Kobett,
Midwest Research Institute. July 1964. viii, 67p.
OTS price, $2.00.
(NASA CONTRACTOR REPORT CR-80)

A computer program was developed which is particularly well suited for use in parametric flutter investigations where a large quantity of numerical data is required. The underlying analysis used exact, linearized, three-dimensional aerodynamic theory so the program can be used to investigate the critical low supersonic regime. Finite panel arrays can be treated, and wind-tunnel installations can be simulated. A limited quantity of informative numerical data is presented. Most of the data pertains to the flutter of single panels with free side edges, with and without adjacent vertical side walls.

I. Kobett, D. R.
II. Midwest Research Institute
III. NASA CR-80

NASA

NASA CR-80
National Aeronautics and Space Administration.
RESEARCH ON PANEL FLUTTER. D. R. Kobett,
Midwest Research Institute. July 1964. viii, 67p.
OTS price, $2.00.
(NASA CONTRACTOR REPORT CR-80)

A computer program was developed which is particularly well suited for use in parametric flutter investigations where a large quantity of numerical data is required. The underlying analysis used exact, linearized, three-dimensional aerodynamic theory so the program can be used to investigate the critical low supersonic regime. Finite panel arrays can be treated, and wind-tunnel installations can be simulated. A limited quantity of informative numerical data is presented. Most of the data pertains to the flutter of single panels with free side edges, with and without adjacent vertical side walls.

I. Kobett, D. R.
II. Midwest Research Institute
III. NASA CR-80

NASA

"The aeronautical and space activities of the United States shall be conducted so as to contribute . . . to the expansion of human knowledge of phenomena in the atmosphere and space. The Administration shall provide for the widest practicable and appropriate dissemination of information concerning its activities and the results thereof."

—NATIONAL AERONAUTICS AND SPACE ACT OF 1958

NASA SCIENTIFIC AND TECHNICAL PUBLICATIONS

TECHNICAL REPORTS: Scientific and technical information considered important, complete, and a lasting contribution to existing knowledge.

TECHNICAL NOTES: Information less broad in scope but nevertheless of importance as a contribution to existing knowledge.

TECHNICAL MEMORANDUMS: Information receiving limited distribution because of preliminary data, security classification, or other reasons.

CONTRACTOR REPORTS: Technical information generated in connection with a NASA contract or grant and released under NASA auspices.

TECHNICAL TRANSLATIONS: Information published in a foreign language considered to merit NASA distribution in English.

TECHNICAL REPRINTS: Information derived from NASA activities and initially published in the form of journal articles.

SPECIAL PUBLICATIONS: Information derived from or of value to NASA activities but not necessarily reporting the results of individual NASA-programmed scientific efforts. Publications include conference proceedings, monographs, data compilations, handbooks, sourcebooks, and special bibliographies.

Details on the availability of these publications may be obtained from:

SCIENTIFIC AND TECHNICAL INFORMATION DIVISION

NATIONAL AERONAUTICS AND SPACE ADMINISTRATION

Washington, D.C. 20546